Human Umbilical Cord Mesenchymal Stem Cell-derived Extracellular Vesicles Ameliorate Airway Inflammation in a Rat Model of Chronic Obstructive Pulmonary Disease (COPD)

Noridzzaida Ridzuan
Universiti Sains Malaysia
Norashikin Zakaria
Universiti Sains Malaysia
Darius Widera
University of Reading
Jonathan Sheard
University of Reading
Mitsuru Morimoto
RIKEN Centre for Developmental Biology
Hirofumi Kiyokawa
RIKEN Centre for Developmental Biology
Seoparjoo Azmel Mohd Isa
Universiti Sains Malaysia
Gurjeet Kaur Chatar Singh
Universiti Sains Malaysia
Kong-Yong Then
Cryocord Sdn Bhd
Ghee-Chien Ooi
Cryocord Sdn Bhd
Badrul Hisham Yahaya (badrul@usm.my)
Universiti Sains Malaysia https://orcid.org/0000-0002-3295-9676

Research

Keywords: COPD, umbilical cord mesenchymal stem cells, extracellular vesicles, animal model

Posted Date: August 4th, 2020

DOI: https://doi.org/10.21203/rs.3.rs-49230/v1

Version of Record: A version of this preprint was published on January 12th, 2021. See the published version at https://doi.org/10.1186/s13287-020-02088-6.

Abstract

Chronic obstructive pulmonary disease (COPD) is an incurable and debilitating chronic disease characterized by progressive airflow limitation associated with abnormal levels of tissue inflammation. Therefore, stem cell-based approaches to tackle the condition are currently a focus of regenerative therapies for COPD. However, stem cell-based therapies are cumbersome and often associated with high costs. Extracellular vesicles (EV) released by all cell types are crucially involved in paracrine, extracellular communication. Recent advances in the field suggest that stem cell-derived EV possess a therapeutic potential which is comparable to the cells of their origin. In this study, we assessed the potential anti-inflammatory effects of human umbilical cord mesenchymal stem cell (hUC-MSC) derived EV in a rat model of COPD. EV were isolated from hUC-MSC and characterized by the transmission electron microscope, western blotting, and nanoparticle tracking analysis. As a model of COPD, male Sprague Dawley rats were exposed to cigarette smoke for up to 12 weeks followed by transplantation of hUC-MSC or application of hUC-MSC-derived EV. Lung tissue was subjected to histological analysis using hematoxylin and eosin staining, alcian blue-periodic acid Schiff (AB-PAS) staining, and immunofluorescence staining. Gene expression in the lung tissue was assessed using microarray analysis. Both, transplantation of hUC-MSC and application of EV resulted in a reduction of peribronchial and perivascular inflammation, alveolar septal thickening associated with mononuclear inflammation, as well as a decreased number of goblet cells. Moreover, hUC-MSC and EV ameliorated the loss of alveolar septa in the emphysematous lung of COPD rats and reduced the levels of NF-κB subunit p65 in the tissue. Subsequent microarray analysis revealed that both hUC-MSC and EV significantly regulate multiple pathways known to be associated with COPD. In conclusion, we show that hUC-MSC-derived EV effectively ameliorate by COPD-induced inflammation. Thus, EV could serve as a new cell-free based therapy for the treatment of COPD.

Introduction

The pathogenesis of the chronic obstructive pulmonary disease (COPD) is characterized by chronic inflammation that leads to small airway obstruction and emphysema (Li *et al.*, 2015). 80 to 90% of all COPD cases are caused by exposure to cigarette smoke (CS) (Churg, Cosio & Wright, 2008). Inhalation of CS increases the number of neutrophils, B cells, macrophages, and $CD8^+$ T cells in the small airway and lungs. These cells, in turn, release multiple inflammatory cytokines, proteinases, and chemokines that together contribute to the degeneration of lung parenchyma (Shapiro, 1999; D'Agostino *et al.*, 2010). Symptoms of COPD include chronic cough, dyspnea, and excessive production of sputum while anorexia, fatigue and weight loss may present in patients with severe COPD (Celli, MacNee & Force, 2004).

Mesenchymal stem cells (MSC) are multipotent stem cells capable of differentiating into osteoblasts, adipocytes and chondroblasts lineages (Dominici *et al.*, 2006). Apart from bone marrow (BM), MSC can be isolated from various tissue including umbilical cord (UC), placenta, adipose tissue (AT), amniotic fluid, and lung tissue (Liu, Fang & Kim, 2016). However, UC represents an attractive source of MSC as UC-MSC is less ethical concern like embryonic stem cells and the isolation of UC-MSC is non-invasive as

compared to BM-MSC. Moreover, UC-MSC exhibit the highest proliferation rate and clonality, and slower senescence rate as compared to BM-MSC, and AT-MSC (Jin *et al.*, 2013).

In addition to MSC differentiation capability, its regenerative capacity includes the ability to ameliorate the inflammatory response as the potential therapeutic tool in regenerative medicine. Multiple pre-clinical studies suggest that MSC have the potential to ameliorate the symptoms of many lung diseases such as pulmonary hypertension, asthma, COPD, and pulmonary fibrosis (Lee *et al.*, 2012; Zeng *et al.*, 2015; Gu *et al.*, 2015; Dong *et al.*, 2015). In the animal model of smoke-induced pulmonary emphysema, biweekly administration of adipose-derived MSC cells decreases the level of inflammation, apoptosis, and alveolar enlargement (Schweitzer *et al.*, 2011). The result from the first phase of clinical trials also demonstrates MSC to be safe when administered in COPD patients while reducing the C-reactive protein at one month after transplantation (Weiss *et al.*, 2013).

Studies have shown the important function of paracrine factors including growth factor, cytokines, and extracellular vesicles (EV) in mediating MSC therapeutic effects. Recently, an increasing number of researches have focused on studying the therapeutic effects of EV in various diseases. EV are small membrane vesicle of multivesicular bodies heterogeneous in size released by a variety of cell types including MSC. EV can be found in body fluids such as milk, saliva, urine, amniotic fluid and cerebrospinal fluid. There are two commonly studied EV which are exosomes and microvesicles. Exosomes size ranging from 40-100nm originated from the inward budding of endosome that forms multivesicular bodies (MVB) and released when the MVB fused with the cell membrane (Sarko & McKinney, 2017). While microvesicles (MV) also known as shed microvesicles size ranging from 50 to 1000nm are formed by outward budding of the cell membrane (Rani *et al.*, 2015). The isolation of EV can be conducted via various methods including differential ultracentrifugation, density-gradient separation, and immunoaffinity capture (Greening *et al.*, 2015). The cargo of EV are proteins, lipids, messenger ribonucleic acid (mRNA) and micro RNA (miRNA) which act as messenger molecules in intercellular communication (Ludwig & Giebel, 2012; Yu, Zhang & Li, 2014).

Studies have shown that EV isolated from MSC mimics the therapeutic effects of MSC, participating in immunomodulation and regeneration in many animal models. MSC-EV have been reported to reduce the infarct size in mice model of myocardial ischemia/reperfusion injury (Lai *et al.*, 2010). MSC-EV were also capable of alleviating inflammation by reducing IL-1β, while increasing the IL-10 expression, reduced mRNA and protein levels of p65, TNF-α, inducible nitric oxide synthase (iNOS), cyclooxygenase-2. Reduction of oxidative stress markers such as malondialdehyde (MDA), and myeloperoxidase (MPO), and increased superoxide dismutase (SOD), and glutathione (GSH) were observed. Apoptosis was also markedly reduced when treated with MSC-EV by decreasing the cleavage of caspase-3, caspase-8, and caspase-9 (Yang *et al.*, 2015). Besides, the use of EV has been recently suggested as a potential treatment option for COPD (Kadota *et al.*, 2016; O'Farrell & Yang, 2019). However, to our knowledge, no attempts have yet been made to compare the impact of MSC transplantation to EV administration for in vivo models of COPD. In this study, we examined the impact of human umbilical cord MSC (hUC-MSC) and hUC-MSC derived EV on inflammation, airway remodelling, and emphysema in a rat model of COPD.

In this study, we opted to use cigarette smoke to induce the inflammation in COPD 2 times/day, 7 days/week for 12 weeks following method from Zheng et al., (2009) with slight modification. 12 weeks cigarette smoke exposure were chosen as our model as inflammation, increased goblet cell count, and emphysema were readily observed in this 12 weeks model (Zheng *et al.*, 2009).

Materials And Methods

Preparation of FBSEV deprived medium

DMEM/F12 (Thermofisher Scientific, USA) supplemented with 10% FBS (Thermofisher Scientific, USA) were subjected to ultracentrifugation at 100,000 x g at 18 hours at 4^{o}C by using Type 50.2Ti fixed-angle rotor, Optima L-100K Ultracentrifuge (Beckman Coulter, USA). Medium was collected and supplemented with 1% antibiotic antimycotic containing penicillin, streptomycin and amphotericin B (Thermofisher Scientific, USA), and 1% L-glutamine (Thermofisher Scientific, USA).

Cell culture, generation of conditioned media (CM) and isolation of EV

Human umbilical cord-derived MSCs (hUC-MSC) passage 4 was kindly provided by Cryocord Sdn Bhd (https://cryocord.com.my/). Cell preparation were conducted in Current Good Manufacturing Practice (cGMP) accredited laboratory. The Wharton's jelly umbilical cord were shredded and enzymatically digested using collagenase (Worthington Biochem, USA) for approximately 2 hours at 37°C. The mesenchymal cells were isolated from Wharton's jelly by passing the tissue through a syringe and needle. hUC-MSC were cultured in Dulbecco's modified Eagle's medium (DMEM) - low glucose (Gibco,USA) supplemented with 10% human serum, and 100U/ml penicillin and 100µg/ml streptomycin and 0.25µg/ml amphotericin (Gibco,USA). The hUC-MSC were cryopreserved using standard cryopreservation protocol until being used in the following research experiment.

hUC-MSC were characterized using flow cytometric analysis, and multilineage differentiation capacity according to International Society for Cellular Therapy (ISCT) criteria for MSCs (Witwer *et al.*, 2019). Positive cell surface markers CD90, CD105, CD73, CD166, and HLA-ABC and negative for hematopoietic markers of CD34, CD45, HLA-DR were characterized using flowcytometry analysis. Manwhile multilineage differentiation adipogenesis, osteogenesis, and chrondrogenesis were conducted using commercially available differentiation kit.

hUC-MSC-CM were obtained from hUC-MSC passage 5 to passage 7. hUC-MSC were cultured from a density of 4000 cells/cm^2 in complete medium, made up of DMEM/F12 (Thermofisher Scientific, USA) supplemented with 10% FBS (Thermofisher Scientific, USA), 1% antibiotic antimycotic containing penicillin, streptomycin and amphotericin B (Thermofisher Scientific, USA), 1% L-glutamine (Thermofisher Scientific, USA), and 20ng/mL basic fibroblast growth factor (bFGF) (Thermofisher Scientific, USA) and incubated at 37^{o}C, in humidified air with 5% CO_2. After 48 hrs of culture, media was changed to complete

medium for the generation of hUC-MSC conditioned media (hUC-MSC-CM). After 72 hours, hUC-MSC-CM was collected and concentrated using Amicon® Ultra-15 Centrifugal Filter Devices (Merck Millipore, USA).

For the generation and isolation of hUC-MSC-EV, hUC-MSC were similarly cultured as described above. After 48 hours, the media was changed to FBSEV-deprived complete medium. After 72 hrs, hUC-MSC-CM was collected and subjected to differential centrifugation. First, centrifugation of hUC-MSC-CM was conducted by using Kubota 2420 Compact Tabletop Centrifuge (Kubota, Japan) at 300xg for 10 mins to remove dead cells. The supernatant was collected and centrifuged again by using Allegra X-15R Centrifuge Ultracentrifuge (Beckman Coulter, USA) at 10,000xg for 30 mins to remove debris, followed by ultracentrifugation at 100,000xg for 2 hrs to precipitate the hUC-MSC-EV by using Type 50.2Ti fixed-angle rotor, Optima L-100K Ultracentrifuge (Beckman Coulter, USA). The supernatant was discarded and the hUC-MSC-EV pellet was washed by resuspending in 1xPBS then re-pelleted by ultracentrifugation for 1 hr. The hUC-MSC-EV pellet was collected and resuspended in 150µL 1xPBS and used fresh for the treatments.

Transmission Electron Microscope

Freshly isolated hUC-MSC-EV in 150µl of 1xPBS suspension were loaded onto carbon-coated copper grids (Ted Pella, USA) and incubated for 10 minutes. The grid was blotted with filter paper and stained with 2% Uranyl acetate (Ted Pella, USA) for 1 minute. Excessive uranyl acetate was removed and the grid was let dry for 15 min before viewing using Energy Filter TEM Libra-120 (Carl Zeiss AG, Germany).

Nanoparticle tracking analysis

The particle size of hUC-MSC-EV was characterized by nanoparticle tracking analysis (NTA) using a NanoSight NS300 (Malvern analytical, United Kingdom) blue laser system. hUC-MSC-EV were diluted with 1xPBS between 1:10 and 1:20 and loaded into the laser module sample chamber. The system focuses the laser beam allowing observing and measuring small particles. Five readings were recorded for each hUC-MSC-EV sample.

Western blot

β-actin and CD63 expression were confirmed with western blot analysis. 2mg/mL of hUC-MSC-EV were separated by using 12% SDS-polyacrylamide gel electrophoresis (PAGE) and then transferred onto polyvinylidene difluoride (PVDF) membrane (Bio-rad). The membrane was blocked with 2% BSA for 1 hour at room temperature and incubated with primary antibodies, rabbit monoclonal antibody CD63 (Abcam) 1:2000 dilution, and rabbit monoclonal antibody β-actin (Cell Signalling Technologies) 1:5000 dilution overnight at 4^{o}C. The membrane was then washed with PBST and incubated with fluorescence secondary antibody goat polyclonal anti-rabbit IgG (Thermo Fisher Scientific) 1:10000 dilution for 1 hour at room temperature. The secondary antibodies were washed with PBST and developed using a fluorescence detection system (Licor).

Animal model of COPD

Male Sprague Dawley (SD) rats aged 8-9 weeks (n=36) were obtained from the Animal Research and Service Centre (ARASC), Universiti Sains Malaysia. All animal procedures were approved and performed according to the ethical standards of the Animal Ethics Committee of the Universiti Sains Malaysia [No. USM / Animal Ethics Approval/2016/(104)(812)]. The *in vivo* study were conducted in GLP accredited laboratory in Animal Research Facilities, Advanced Medical and Dental Institute (IPPT), Universiti Sains Malaysia. The experimental procedure was conducted as previously described by Zheng et al., (2009) with slight modifications. COPD symptoms and inflammation were established by using commercially available cigarettes, Marlboro (Philip Morris, USA) (each containing 10.0 mg of tar and 1.0 mg of nicotine). In total, 36 rats were divided into 6 groups (n=6); naïve (untreated group), CS (injury group), CSSH (2 week self-healing group), hUC-MSC-EV (hUC-MSC-EV treated group), hUC-MSC (hUC-MSC treated group), and hUC-MSC-CM (hUC-MSC-conditioned media treated group). All groups except naïve were exposed to side-stream cigarette smoke for 15 minutes per session, 6 cigarettes for 2 sessions, 7 days a week, for 12 weeks in a smoking chamber. Rats were left to rest for 2 hours between each session.

Treatments were given via intratracheal delivery in 150µL vehicle (1xPBS) on day 85 post cigarette induction. Rats were anaesthetized intravenously by using ketamine (50mg/kg) xylazine (5mg/kg). hUC-MSC ($2.5x10^6$), hUC-MSC-EV isolated from $2.5x10^6$ hUC-MSC, and hUC-MSC-CM concentrated from $2.5x10^6$ hUC-MSC were used in the experiment. Naïve and CS groups were euthanized on day 85, meanwhile, the rest of the groups were euthanized on day 99. Rats were euthanized by using intravenous injection of pentobarbital (200mg/mL) (Dolethal, Lure Cedex, France).

Peripheral blood collection

Peripheral blood (300µl) was collected from rat tail vein and placed into a 1ml EDTA tube (Greiner bio-one, Austria) and subjected to whole blood count using Cell Dyn Hematology Analyzer (Abbott, USA).

Histological assessment

Hematoxylin and eosin (H&E) staining was performed for the analysis and scoring of peribronchial and perivascular inflammation, alveolar inflammation, and emphysema. Meanwhile, alcian blue – periodic acid schiff (AB-PAS) staining was performed for the analysis of goblet cell count. Scoring of inflammation within the airway was conducted using a semi-quantitative analysis. Slides were blindly coded before the tissues were scored by a pathologist. The inflammation scoring was performed using the scale of 0 to 3 based on the presence and intensity of inflammatory cell infiltration in the peribronchial and perivascular area. Two slides were analysed per animal with a total of 5 animals per group. The score was done according to the parameters: 0, no inflammation detected; 1, occasional cuffing with inflammatory cells; 2, most bronchi and vessels are surrounded by a thin layer of inflammatory cells (1-5 cells thick), and 3, most bronchi and vessels are surrounded by a thick layer of inflammatory cells (>5 cells thick). Alveolar inflammation scoring was done by grid on tissue section photos captured by fluorescence microscopy (Olympus, Japan). 100 points were counted on random

areas on the slides. 10 areas were analysed on 2 slides per animal with a total of 5 animals per group. Goblet cells were counted using light microscopy (Olympus, Japan). 500 cells were counted and the number of goblet cells was divided by total cells to get a percentage of goblet cells. One slide per animal with a total of 5 animals per group were assessed. Emphysema was assessed by using mean linear intercept (Lm) which measures the enlargement of alveolar space. Measurement was done by using 40x objective and 10x eyepiece, and photos of the sections were taken and superimposed with 30x30μm grid. Ten photos of 2 slides per animal with a total of 5 animals per group were captured. The number of alveolar intercepts along the gridline were counted and calculated based on the following formula as described previously (Choe et al., 2003):

$$Lm = \frac{NL}{m}$$

where;

N = number of lines across the photographed area

L = length of the line across the photographed area

m = number of intercepts

RNA extraction and microarray analysis

RNA extraction was performed on 30mg of rat lung from Naïve, CS, hUC-MSC, and hUC-MSC-EV groups using the RNeasy Mini Kit (Qiagen, Germany) following the manufacturer's instructions. The purity and concentration of RNA were measured by NanoDrop ND1000 (Thermo Fisher Scientific, US). RNA integrity was determined by Agilent RNA 6000 Nanokit (Agilent Technology, US). cDNA was synthesized and hybridized at 65^{o}C for 17 hours and viewed using Agilent SureScan Microarray Scanner (Agilent Technology, US). Comparison between different sample dataset was normalised and analysed using Gene Spring software. The sample datasets were subjected to t-test to identify significant changes (p<0.05) between the sample and control group. Genes with p<0.05 and fold-change >2.0 were filtered as significantly regulated. Volcano plot, heat map, principle component analysis, venn diagram, and pathway analysis were generated using Gene Spring software. Gene Ontology analysis using Panther (www.pantherdb.org) was used to classify differential expression analysis (DEG) by its functional role. GO terms with p<0.05 was considered significantly enriched by DEG.

Immunofluorescent staining

Immunofluorescent staining was performed to study the expression of NF-κB subunit p65. Briefly, tissue sections were deparaffinized in xylene and rehydrated in graded ethanols. The tissues were blocked with 5% goat serum for 30 min and incubated with primary antibody mouse monoclonal NF-κB-P65 (F-6) (Santa Cruz Biotechnology, USA) 1:200 for 1.5 hours in room temperature. After washing with PBS, slides

were incubated with secondary antibody Alexa Fluor 555 goat anti-mouse IgG (H+L) (Thermo Fisher Scientific, USA) and counterstained with DAPI 1:2000 in 1xPBS, and viewed under IX71 Fluorescence Microscope (Olympus, Japan).

Statistical analysis

Statistical analyses were performed using GraphPad Prism 7 version 7.0 (GraphPad Software, USA). Comparison among more than 2 groups were done using one-way analysis of variance (ANOVA) with Tukey's multiple comparison test. Data presented as median ± standard deviation (SD). Differences are considered to be statistically significant when $p \leq 0.05$, whereas $p \leq 0.001$ was considered to be highly significant.

Results

Characterization of hUC-MSC

MSCs were isolated from human umbilical cord blood were subjected to immunocytochemistry and differentiation analysis. hUC-MSC were positive for CD73, CD90, CD105, and CD166, and negative for CD34, CD45, CD31, and HLA DR DP DQ (Table 1). Differentiation analysis showed the ability of MSC to differentiate into adipocyte evidenced by lipid droplet formation, osteocyte evidenced by calcification formation, and chondrocyte evidenced by cell matrix formation – Fig 1.

Table 1: Expression analysis of hUC-MSC surface marker

Surface marker	Expression (%)
CD73	92.4
CD90	93.1
CD105	84.1
CD45	0.2
CD34	0.0
CD31	0.2
CD166	63.1
HLA-ABC	60.9
HLA DR DP DQ	0.0

Characterization of hUC-MSC-EV

hUC-MSC-EV were isolated by differential centrifugation to remove cell debris and apoptotic bodies. hUC-MSC-EV pallet suspended in 1xPBS was characterized based on morphology, size distribution and protein

marker expression. Energy filtered transmission electron microscopy examination showed hUC-MSC-EV were rounded in shape with the average size of 200nm (Fig. 2A). Western Blot analysis showed the presence of the specific exosome marker CD63 at 30-65kDa and β-actin at 42kDa (Fig. 2B). Nanoparticle tracking analysis of hUC-MSC-EV showed an average diameter of 153nm (Fig. 2C). Table 2 shows the mean, mode, SD and range of 3 hUC-MSC-EV samples used in NTA.

Table 2: Analysis of hUC-MSC-EV size distribution

Sample	Mean (nm)	Mode (nm)	SD (nm)	Range (nm)
1	141.2	115.0	51.4	36-737
2	156.5	116.9	68.4	64-795
3	163.0	123.1	68.3	25-740

hUC-MSC-EV decreased lymphocyte count in peripheral blood

To study the effect of hUC-MSC-EV on the circulating immune cells, peripheral blood was collected and subjected to full blood count. CS exposure for 12 weeks observed a non-significant increase in white blood count (WBC) count with no reduction seen following a 2 weeks self-healing rest period without exposure to CS (CSSH). treatment with hUC-MSC-EV and hUC-MSC-CM did not reduce WBC counts, however, a non-significant decrease was seen in response to hUC-MSC. Notably, CS significantly increased the percentage of lymphocytes compared to the naïve group with no observed mitigation following 2 weeks of self-healing (CSSH). A significant decrease in the percentage of lymphocytes was seen in response to treatment with whole-cell hUC-MSC (*p<0.05), whereas a slight non-significant decrease in response to hUC-MSC-EV and hUC-MSC-CM (Fig. 3).

hUC-MSC-EV reduce the infiltration of the immune cells in the lung

The accumulation of immune cells (neutrophils, eosinophils, lymphocytes and macrophages) in the lung is a key marker for the development of chronic inflammation in COPD. Our result showed that CS caused an influx of these immune cells into the lung (Fig. 4), predominantly neutrophils and macrophages, while lymphocytes and eosinophils remained present at low levels. Two weeks of self-healing (CSSH) failed to reduce the infiltration of all cell types examined. Notably, administration of hUC-MSC-EV, hUC-MSC, and hUC-MSC-CM was significantly reduced the immune cells influx as compared to the CS group.

hUC-MSC-EV alleviates airway inflammation.

Histological scoring and analysis of CS effects on the rat airway and lung parenchyma showed an increase in inflammation scores in response to CS (Fig 5A-B). The accumulation of immune cells significantly increased in the lung parenchyma. Meanwhile, 2 weeks of self-healing (CSSH) did not reduce the inflammation. However, there was a significant reduction of inflammation scores observed in the

parenchyma following treatment with hUC-MSC-EV, whole-cell hUC-MSC, and hUC-MSC-CM (**p<0.001, ***p<0.0001) – Fig 5C-D.

hUC-MSC-EV, hUC-MSC, and hUC-MSC-CM decreased mucus production

To assess mucus overproduction, semi-quantitative histological analysis was conducted to count the incidence of goblet cells between groups. Histological sections of bronchi were stained with AB-PAS where the cell nucleus was stained blue, while goblet cells stained magenta (Fig 6A). Statistical analysis shows that treatment of CS groups with MSC had significantly reduced the number of goblet cells (p<0.05) as compared to CS and self-healing (CSSH), and far better than groups received treatments with hUCMSC-EV and hUCMSC-CM Fig 6B.

hUC-MSC-EV decreased emphysema

To study the effect of CS and treatment intervention on emphysema, the mean linear intercept of alveolar pores were measured on H&E histological slides (Fig. 7A). Quantitative analysis showed that 12 weeks of CS exposure caused alveolar destruction with a significant increase in the mean linear intercept of alveolar pores (Fig 7B), whilst 2 weeks of self-healing failed to mitigate these effects (CSSH). However, a significant (*p<0.05) reduction in the mean linear intercept of the alveolar pores and restoration of tissue was observed following treatment with hUC-MSC-EV. Meanwhile, a non-significant reduction was observed in hUC-MSC, and hUC-MSC-CM.

hUC-MSC-EV decreased the levels of p65 in lung tissue

p65 is a subunit of the prototypic, pro-inflammatory transcription factor NF-κB. Translocation of p65 to the nucleus of a cell is indicative of the cells pro-inflammatory response. To study the translocation of p65 into the nuclei of cells, IHC stained and imaged lung tissue sections was quantified following CS and treatment intervention. A significant increase in the percentage of p65 positive cells was observed in the CS group. Following two weeks of self-healing, a significant reduction of p65 was observed. Treatment with hUC-MSC-EV, hUC-MSC and hUC-MSC-CM further reduced the p65 expression in CS-exposed lung – Fig 8.

CS, hUC-MSC-EV and hUC-MSC alter the gene expression

Our microarray analysis aimed to determine the pathways and the differential gene expressions altered in CS-induced inflammation lung and in the treatment group (hUC-MSC-EV and hUC-MSC). Differentially expressed genes (DEG) which has been upregulated or downregulated more than the two-fold difference (p<0.05) are considered significant for further investigation to understand the biological, cellular and molecular functions. CS exposure was shown to lead to a total of 17689 DEG, while treatment with HUC-MSC-EV and hUC-MSC are shown to have led to 15160 and 23485 DEG respectively (Fig 9A). Heatmap shows different regulation of DEG from CS group as compared to Naïve, hUC-MSC-EV, and hUC-MSC groups (Fig 9B). PCA plot shows cluster of samples (n=2) in CS, hUC-MSC-EV, and hUC-MSC groups, but high variation was observed in Naïve group (Fig 9C). Volcano plot shows DEG in CS, hUC-MSC-EV, and

hUC-MSC groups (Fig 9D). Venn diagram shows overlapping DEG among CS, hUC-MSC-EV, and hUC-MSC (Fig 9E). 9888 DEG were overlapped in 3 groups, 1610 DEG were overlapped between CS and hUC-MSC-EV, 4597 DEG were overlapped between CS and hUC-MSC, and 1976 DEG were overlapped between hUC-MSC-EV and hUC-MSC.

Gene Ontology analysis

GO Slim analysis of the biological process was performed on the DEG results presented in the tables below. The enriched GO terms were identified in CS (**Suppl 1 Table A**) hUC-MSC (**Suppl 1 Table B**) and hUC-MSC-EV (**Suppl 1 Table C**) groups. The GO terms for the CS group are related to the regulation of the cellular process, regulation of catalytic activity, regulation of signalling, and regulation of the metabolic process. While GO terms for hUC-MSC-EV are related to the regulation of catalytic activity, movement of cell or subcellular component, regulation of signalling, regulation of cell communication, cellular protein modification process, and regulation of RNA metabolic process. GO terms for hUC-MSC are related to chemical synaptic transmission, sensory perception of chemical stimulus, G-protein coupled receptor signalling pathway, regulation of signalling, regulation of cell communication, ion transport, regulation of biological quality, developmental process, and ribosome biogenesis.

Pathway analysis

Pathways related to COPD with a significance value of $p<0.05$ were considered to be significantly up or downregulated. 38 pathways were significantly regulated in response to CS. Whereas, following hUC-MSC-EV treatment, 58 pathways were significantly regulated, and only 17 pathways were significantly regulated following treatment with UCMSC. The notable pathways which were highly regulated in the CS and hUC-MSC-EV groups include; TGF-β receptor signalling pathway, IL-4 signalling pathway, and TNF-alpha NF-kB signalling pathway. Meanwhile, pathways which were highly regulated in response to the UCMSC group include; TNF-alpha NF-kB signalling pathway, senescence and autophagy pathway, and IL-9 pathways. All the significantly regulated pathways are shown in **Suppl 2**.

Gene expression

We look for the highest frequency of genes that are expressed in pathways in injury (CS) and treatment (hUC-MSC and hUC-MSC-EV) groups. **Table 3** shows 10 genes with the highest frequency in CS. NFKB1 and Mapk1 are expressed in 11 pathways, followed by Jun and Map2k1 which are expressed in 10 pathways. **Table 4** shows 8 genes with the highest frequency in hUC-MSC-EV group. Akt1 is expressed in 22 pathways, meanwhile, Mapk1, NFKB1, Map2k1 are expressed in 18 and 15 pathways respectively. **Table 5** shows 8 genes with the highest frequency in UCMSC group. Akt1 and Mapk1 are expressed in 6 pathways, while Map2k1 and TGFB1 are expressed in 5 and 4 pathways respectively.

Table 3: Genes with the highest frequency in CS group.

Genes	P value	FC	Frequency
Nfkb1	0.0015	6.0905	11
Mapk1 (ERK2)	0.0268	-2.841	11
Jun	0.0262	-2.592	10
Map2k1 (MEK1)	0.0097	3.2654	10
Mapk9	0.0026	-4.401	9
Crebbp (CBP)	0.0089	-4.07	8
Prkcz	0.0098	3.6678	8
p65	0.0017	6.3732	7
Grb2	0.0235	-2.237	7
Src	0.0115	-2.948	7

Table 4: Genes with the highest frequency in hUC-MSC-EV group.

Gene	P value	FC	Frequency
Akt1	0.00172	-4.53957	22
Nfkb1	0.003537	-4.44685	18
Map2k1	0.003896	-3.49505	15
Pik3r1	0.002295	5.379887	15
Mapk1	0.006903	4.221682	14
Grb2	0.003507	-3.40208	12
Prkcz	0.006365	-3.68258	10
p65	0.001438	-5.04044	10

Table 5: Genes with the highest frequency in hUC-MSC group.

Gene	P value	FC	Frequency
Tgfb1	0.024022	-5.81517	6
Akt1	0.004107	-6.88884	6
Mapk1	0.004209	4.946711	5
Pik3r1	0.001114	9.6399	4
Map2k3	0.002436	-4.57343	4
Mapk3	0.01819	2.465821	4
Mapk8	0.006342	-3.81553	4
Map2k1	3.85E-04	-9.33631	4

Discussion

Our study aimed to determine the effects of hUC-MSC-EV in comparison to hUC-MSC for the treatment of COPD. The therapeutic potential of MSC and MSC derived secreted factors have been widely demonstrated in various diseases, including rheumatoid arthritis, asthma, and Crohn's disease (Gonzalez-Rey *et al*., 2010; Song *et al*., 2015; Panes *et al*., 2016). In COPD, MSC capabilities to mitigate inflammation has been tested in the preclinical and clinical setting around the world (Weiss *et al*., 2013; Liu, Fang & Kim, 2016; Bich *et al*., 2020). However, little is known about the effect of extracellular vesicles isolated from MSC for the treatment of inflammation in COPD. hUC-MSC used in this study were positive for CD73, CD90, CD105, and CD166, and negative for CD34, CD45, CD31, and HLA DR DP DQ as previously described by Witwer *et al*., 2019. Meanwhile differentiation analysis showed the ability of hUC-MSC to differentiate into adipocyte, osteocyte, and chondrocyte. hUC-MSC-EV isolated from hUC-MSC showed a rounded morphology with the average of 153nm in diameter, and protein analysis showed a positive marker for CD63 exosomal marker. Following 12 weeks of CS exposure, the evidence of accumulation of inflammatory cell infiltrated in peribronchial and perivascular tissues as well as the parenchyma, goblet cell hyperplasia, expression of p65, and the development of emphysema was consistent to that of previously published studies (Nie *et al*., 2012; Zhang *et al*., 2014) indicating the development of COPD by CS inhalation. Two weeks of self-healing was significantly reduced the expression of p65, but did not reduce the inflammation and remoduelling the destruction of alveolar in the lung. The treatment of hUC-MSC-EV, hUC-MSC, as well as hUC-MSC-CM were significantly reversed the effect of sidestream CS on lung inflammation, expression of p65, and emphysema. Our study on microarray also revealed that CS was significantly regulated pathways related to COPD and upregulated genes related to inflammation including NFKB1, p65, and protein kinase Cζ (PRKCZ), whilst treatment with hUC-MSC-EV and hUC-MSC were observed to reverse these CS-induced gene expression effects.

Cigarette smoke is the main risk factor of COPD with over 80% of all COPD cases attributed to cigarette smoking, therefore cigarette smoke is widely employed by the researchers to develop the *in vivo* COPD

model over other inducers such as biomass fuel, lipopolysaccharide, and elastase (Borzone *et al.*, 2007; Al Faraj *et al.*, 2014; He *et al.*, 2017; Ghorani *et al.*, 2017). To establish COPD model in animal, many studies had employed cigarette smoke exposure for 6 months period that showed much severe injury in the lung (Huh *et al.*, 2011; Kim *et al.*, 2016). However, there are studies which employed 12 weeks cigarette smoke exposure demonstrated characteristic of COPD including inflammation, airway remodelling, fibrosis, goblet cell hyperplasia, and emphysema (Gu *et al.*, 2015; He *et al.*, 2015). This method is more feasible for *in vivo* study as compared to 6 months period which is time-consuming. Our study is in agreement with the previous studies that showed 12 weeks of cigarette smoke exposure is sufficient to induce characteristics similar to COPD in SD rats. Importantly, our method of CS exposure for 2 times/day, 7 days/week for 12 weeks exposure induced the emphysema in rat lung, a characteristic of the chronic model of COPD (Leberl, Kratzer & Taraseviciene-Stewart, 2013). It should be noted that animal models do not fully mimic human condition, and regardless types of animal used and the duration of cigarette smoke exposure, the severity of the injury are only equivalent to the Global Initiative for Obstructive Lung Disease (GOLD) stage I or II diseases (Fricker et al., 2014).

COPD is characterized by airway and parenchymal inflammation that leads to mucus overproduction and emphysema, although these characteristic may not present in all patients, as the emphysematous lung only occurs in 20% of all COPD patients (Churg, Cosio & Wright, 2008; Akram *et al.*, 2012). Nevertheless, in the animal model, the presence of emphysema is one of the important characteristics to confirm the development of COPD (de Oliveira, 2016). On the other hand, mucus overproduction is considered difficult to reproduce in the rat model due to the low number of goblet cells in the bronchi (Churg, Cosio & Wright, 2008). Our study using CS exposure for 12 weeks in SD rats successfully developed characteristic of COPD as we can observe the increased influx of immune cells indicating the development of inflammation in the lung, increased goblet cells count which shows increase mucus production, and increased mean linear intercept which shows the development of emphysema.

Airway inflammation begins with the disruption of the airway and vascular function, allowing infiltration of immune cells in the lung (Schweitzer *et al.*, 2011; Presson Jr *et al.*, 2011). In the acute phase of CS exposure that lasts until the second week, increased of neutrophils was observed. After the second week, macrophage begins to increase, and neutrophils start to decrease but not fully resolve, indicating chronic inflammation began to develop (Stevenson *et al.*, 2007). In our study, the increased in neutrophils, eosinophils, lymphocytes, and macrophages counts were observed, however, neutrophils and macrophages are the predominant immune cells infiltrating the lung. Our results also showed immune cells accumulation was observed more prominently in the alveolar area rather than the peribronchial and perivascular area which destroy the alveolar wall leading to the emphysematous lung.

The accumulation of immune cells in alveolar walls are prerequisite for the development of emphysema. Neutrophils elastase (NE) was reported to induce the epithelial apoptosis and emphysema, meanwhile excessive MMP-9 released by macrophage can result in permanent alveolar destruction (Atkinson *et al.*, 2011; Hou *et al.*, 2014). Shapiro et al., (2003) was demonstrated that crosstalk between these two cells is crucial in the development of emphysema. The presence of neutrophils is crucial as neutrophils release

NE that is required to recruit more neutrophils and monocytes into the lung. The study was also reported that mice deficient of NE ($NE^{-/-}$) has shown significantly protected from the development of emphysema. Shapiro and colleagues further proved that the synergistic effects of neutrophil and macrophage are required to enhance the potency of both cells. The absence of NE causes the tissue inhibitors of metalloproteinases (TIMPs) to inhibit the action of macrophage elastase. Likewise, the absence of macrophage elastase caused an increased in α-1 anti-trypsin, a major inhibitor of NE. Thus, the presence of both neutrophils and macrophages are an important factor in the development of emphysema (Shapiro *et al.*, 2003).

CS exposure also causes mucus overproduction, although the symptoms may not present in all COPD patients (Burgel & Martin, 2010). The mechanism by which CS-induced the overproduction of mucus occurs through activation of TNF-α converting enzyme (TACE) which cleaved pro-TNF-α to release TNF-α that activates epidermal growth factor receptor (EGFR) which result in mucin production (Shao, Nakanaga & Nadel, 2004). The accumulation of neutrophils in the lung during CS exposure may also exacerbate the mucus overproduction as neutrophils are also in part responsible for the impaired mucociliary clearance, increased goblet cells count, and excessive mucus production. NE released by neutrophils increased the expression of MUC5AC by enhancing the mRNA stability via reactive oxygen species mechanism (Arai *et al.*, 2010; Fischer & Voynow, 2002). Besides, activation of TNF-α and subsequent activation epidermal growth factor pathway can also stimulate NE to induce the expression of MUC5AC (Kohri, Ueki & Nadel, 2002).

MSC has been actively investigated as a potential therapy for COPD. Clinical studies measuring C-reactive protein in COPD patient revealed the benefit of MSC administration in mitigating the inflammation (Hayes *et al.*, 2020). In the animal model, MSC alleviates the inflammation by reducing the alveolar macrophage, while at the same time promoting the expression of the anti-inflammatory cytokine, IL-10 in macrophages (Gu *et al.*, 2015). MSC also reduced the neutrophil infiltration regardless of the route of administration (Antunes *et al.*, 2014). This therapeutic effects of MSC are governed by the released of paracrine factors including growth factor, cytokine, and EV rather than cell-to-cell contact (Fontaine *et al.*, 2016). Recently, research begins to unravel the therapeutic effects of MSC-EV and better understand the mechanism behind this ability. Several studies have shown anti-inflammatory effects of MSC-EV in mitigating the inflammation similar to MSC. Reduced number of eosinophils, lymphocytes, and airway remodelling were observed in the animal model of asthma when treated with adipose tissue MSC-EV (de Castro *et al.*, 2017). In the rat model of hepatic ischemia-reperfusion injury, hUC-MSC-EV inhibited the activity of the neutrophils by attenuation of respiratory burst and oxidative stress, thus reducing the apoptosis of hepatocytes (Yao *et al.*, 2019). Also, MSC-EV attenuated the pro-inflammatory cytokines such as IL-17, TNF-α, RANTES, MIP1α, MCP-1, CXCL1, HMGB1, while enhancing the production of IL-10, PGE2, and KGF (Stone *et al.*, 2017). Our study demonstrated that hUC-MSC-EV possess anti-inflammatory similar to its cell counterpart, hUC-MSC. The treatment with hUC-MSC-EV significantly reduced immune cells accumulation in the lung especially neutrophils accumulation, reduced emphysema, reduced protein expression of p65, and downregulated DEG related to COPD.

To date, there are no treatment options available to regenerate the lung damage in emphysema. However, stem cell-based therapy demonstrates a promising regenerative capability to restore the function of damaged lung. MSC and MSC-CM are shown to restore the lung function by mitigating the apoptosis in the emphysematous lung (Huh *et al.*, 2011). This anti-apoptosis effect is in part is mediated by vascular endothelial growth factor (VEGF) and VEGF receptor (Guan *et al.*, 2013). In addition, MSC reduced expression of cyclooxygenase-2 in alveolar macrophage, thereby mitigating the emphysema in rat model of COPD (Gu *et al.*, 2015). On the other hand, relatively few studies were conducted to decipher the effects of MSC derived EV in the emphysematous lung. The study by Kim and colleague (2017) comparing the regenerative effects of nanovesicles generated from adipose stem cells (ASC) and ASC derived exosomes in elastase-induced emphysematous lung. The result showed that nanovesicles significantly reduced the emphysema via its cargo content, FGF2, while no significant reduction of emphysema was observed in ASC derived exosome (Kim *et al.*, 2017). Our result provides the evidence of hUC-MSC-EV ability to reduce emphysema in CS-induced COPD in rat model. Considering the importance of neutrophils and macrophages accumulation in the pathogenesis of emphysematous lung, significant reduction in the accumulation of neutrophils when treated with hUC-MSC-EV and hUC-MSC in our study, in part might explain the reduction of emphysema. Decreased in macrophages accumulation were also observed when treated with hUC-MSC-EV, hUC-MSC, and hUC-MSC-CM although the reduction was not significantly different from the injury group. Recent studies also reported MSC derived microvesicles reduced the influx of neutrophils through the effects of KGF (Zhu *et al.*, 2014). However, macrophages are shown to play an important role in MSC anti-inflammatory effects by changing from M1 to M2 phenotype which produces IL-10 that involve in the reduction of inflammation when treated with MSC and MSC-EV (Etzrodt *et al.*, 2012; Gu *et al.*, 2015; Sicco *et al.*, 2017). Although the accumulation of macrophages is prerequisite for emphysema, however, in allergic asthma, depletion of alveolar macrophage reversed the immunosuppressive effect of MSC in which the production of IL-10 was dependent on the presence of alveolar macrophage (Mathias *et al.*, 2013). The macrophages role might explain why macrophages in our study did not significantly reduce as it aids in MSC anti-inflammatory response.

To date relatively few studies examining the effect of MSC in reducing the mucus overproduction. Although there are reports stated that mucus can be mitigated with the administration of MSC, however, in-depth study on the mechanism involve remain unknown (Lee *et al.*, 2011; Mohammadian *et al.*, 2016). In addition, there is no report on the ability of MSC-EV to reduce mucus overproduction. Our study showed a significant reduction of goblet cells count in hUC-MSC. Reduction of goblet cells can be observed in hUC-MSC-EV and hUC-MSC-CM, however, the reduction was not significant. Nevertheless, the details mechanism on how hUC-MSC, hUC-MSC-EV, and hUC-MSC-CM effects on goblet cells are remained unknown and was not elucidated in the current study.

Our microarray analysis was aimed to determine the pathways associated with COPD and gene expression profile in our COPD model. We also seek to understand how the treatment with hUC-MSC-EV and hUC-MSC can change the gene expression profile and pathways in COPD model. Our on DEG analysis of microarray data revealed the importance of p50, p65, and PRKCZ in our animal model. 12 weeks CS exposure significantly upregulated p50, p65, and PRKCZ and the treatment with hUC-MSC-EV

were significantly downregulated the expression of these genes. Immunohistochemistry staining on p65 confirms the significant upregulation of p65 protein in the CS group, and significant downregulation of p65 when treated with hUC-MSC-EV, hUC-MSC, and hUC-MSC-CM. Our study was also revealed that p50, p65, and PRKCZ involved in many pathway regulations that includes TNF-α NF-κβ signaling pathway, IL-2 signaling pathway, oxidative stress, estrogen signaling pathway, and IL-4 signaling pathway.

The expression of PRKCZ and NF-κβ play a vital role in inflammation and thus the pathogenesis of COPD. PRKCZ is upstream of NF-κβ, phosphorylating p65 at serine 311 to promote the acetylation of Lysine 310, thus activating the κβ transcription (Diaz-Meco & Moscat, 2012). Mice deficient of PRKCZ was found to reduce myeloperoxidase and influx of neutrophils, and reduced pro-inflammatory cytokines such as IL-13, IL-17, IL-18, IL-1β, TNF-α, MCP-1, MIP-2, and IFN-γ, while the use of PRKCZ inhibitors blocked the activation of NF-κβ by TNF-α, thus reducing the pro-inflammatory IL-8 expression (Yao *et al.*, 2010; Aveleira *et al.*, 2010). Meanwhile, NF-κβ composed of five members, NF-κβ1 (p50), NF-κβ2 (p52), RelA (p65), RelB, and c-Rel, that regulate a multitude of genes involved in inflammatory responses (Liu *et al.*, 2017). Among all heterodimers of NF-κβ, p50/p65 heterodimer represents the most abundant NF-κβ activated by the canonical pathway (Giridharan & Srinivasan, 2018).

Cigarette smoke activates NF-κβ within one hour of exposure to the lung thus causing inflammatory reactions which increase white blood cell count, lymphocyte count, and granulocyte count (Churg *et al.*, 2003; Flouris *et al.*, 2012). Data from the pre-clinical study showed 4 weeks of CS exposure significantly increased p65 and Iκβα in mice lung as compared to control group (Yu *et al.*, 2018). NF-κβ is also required by IL-1β and IL-17A to induce the expression of MUC5B in bronchial epithelial cells that cause goblet hyperplasia in COPD (Fujisawa *et al.*, 2011). Besides, various studies demonstrated the upregulation of p65 and p50 expression in COPD patients (Di Stefano *et al.*, 2002; Caramori *et al.*, 2003; Tan *et al.*, 2016; Zhou *et al.*, 2018). Microarray study conducted by Yang et al., (2013) revealed the important role of p50 in regulating many pathways of COPD including toll-like receptor signalling pathway, cytokine-cytokine receptor interactions, chemokine signalling pathway, and apoptosis (Yang *et al.*, 2013).

Our study revealed the downregulation of PRKCZ, p65, and p50 expression when treated with hUC-MSC-EV. p50 regulated 18 pathways in hUC-MSC-EV group, while PRKCZ and p65 regulated 10 pathways suggesting the important role of NF-κβ pathway in hUC-MSC-EV therapeutic effects in our model. Downregulation NF-κβ subunit by hUC-MSC-EV can affect multiple pathways in our model thus reducing the inflammation. MSC-EV has been shown to decrease the expression of NF-κβ in *in vitro* model of cystic fibrosis and experimental colitis (Yang *et al.*, 2015; Zulueta *et al.*, 2018). However, much is still unknown about how MSC-EV regulates the NF-κβ pathway. In our study, we did not elucidate the cargo content of EV that is responsible for anti-inflammatory effects on CS-induced lung inflammation. Nevertheless, the study demonstrated that micro-RNA content of MSC derived exosome can reduce p50 NF-κβ pathway in macrophage thus preventing the Toll-like receptor-induced macrophage activation (Phinney *et al.*, 2015). In addition, CCR2 in MSC derived exosomes abolished the ability of CCL2 to induce p65 phosphorylation in macrophages (Shen *et al.*, 2016). Meanwhile, knockdown of GPX-1 in human MSC, reverse the effect of

MSC derived exosomes in reducing the phosphorylation of p65 (Yan *et al.*, 2017). These results proved that multiple cargo contents of MSC-EV play a vital role in mediating the inflammation.

Conclusion

Our study had successfully isolated the hUC-MSC-EV from hUC-MSC. 12 weeks of CS exposure induced the inflammation, increased goblet cells count, and emphysema in the rat model. The treatment with hUC-MSC-EV, hUC-MSC, and hUC-MSC-CM decreased the inflammation in the lung, decreased the goblet cells, and destruction of the lung in rat model of COPD similar to hUC-MSC. hUC-MSC-EV reduced the inflammation in part by expression of PRKCZ, and NF-κβ subunits p65, and p50, which regulates many genes responsible for innate and adaptive immune response. Confirmation study using immunofluorescence on p65 showed similar result as microarray analysis of DEG. Taken together, there are still limited data demonstrating the regenerative and the anti-inflammatory effects of MSC-EV to mitigate the inflammation in COPD. More studies should be conducted to decipher the anti-inflammatory effects of MSC-EV as a whole, as well as exosomes, and microvesicles as different particle might exhibit different therapeutic effects. Determination of cargo content of MSC-EV responsible for the anti-inflammatory effects and the mechanism of action of the cargo content of MSC-EV can provide a clear the ways toward the goal of using hUC-MSC as a new treatment for COPD.

Financial and competing interest disclosure

The study was supported by the Universiti Sains Malaysia (USM) Research University Grant (1001/CIPPT/8012203). The author would like to thank to staff in Dr Darius Widera's lab for helping in hUC-MSC-EV characterisation and western blot analysis and staff in Dr Mitsuru Morimoto's lab for helping in microarray analysis. The authors declare no other financial involvement with any organization or entity with financial interest and/or conflict with matters discussed in the manuscript apart from those disclosed.

References

1. Akram, K. M., Samad, S., Spiteri, M. & Forsyth, N. R. (2012). Mesenchymal stem cell therapy and lung diseases. Mesenchymal Stem Cells-Basics and Clinical Application II. Springer. 2. Al Faraj, A., Shaik, A. S., Afzal, S., Al Sayed, B. & Halwani, R. (2014). MR imaging and targeting of a specific alveolar macrophage subpopulation in LPS-induced COPD animal model using antibody-conjugated magnetic nanoparticles. International journal of nanomedicine, 9, p. 1491. 3. Antunes, M. A., Abreu, S. C., Cruz, F. F., Teixeira, A. C., Lopes-Pacheco, M., Bandeira, E., Olsen, P. C., Diaz, B. L., Takyia, C. M. & Freitas, I. P. (2014). Effects of different mesenchymal stromal cell sources and delivery routes in experimental emphysema. Respiratory Research, 15(1), p. 118. 4. Arai, N., Kondo, M., Izumo, T., Tamaoki, J. & Nagai, A. (2010). Inhibition of neutrophil elastase-induced goblet cell metaplasia by tiotropium in mice. European Respiratory Journal, 35(5), p. 1164-1171. 5. Atkinson, J. J., Lutey, B. A., Suzuki, Y., Toennies, H. M., Kelley, D. G., Kobayashi, D. K., Ijem, W. G., Deslee, G., Moore, C. H. & Jacobs, M. E. (2011). The role of matrix metalloproteinase-9 in cigarette smoke–induced emphysema. American journal of respiratory and critical care medicine, 183(7),

p. 876-884. 6. Aveleira, C. A., Lin, C.-M., Abcouwer, S. F., Ambrósio, A. F. & Antonetti, D. A. (2010). TNF-α signals through PKCζ/NF-κB to alter the tight junction complex and increase retinal endothelial cell permeability. Diabetes, 59(11), p. 2872-2882. 7. Bich, P. L. T., Thi, H. N., Chau, H. D. N., Van, T. P., Do, Q., Khac, H. D., Le Van, D., Huy, L. N., Cong, K. M. & Ba, T. T. (2020). Allogeneic umbilical cord-derived mesenchymal stem cell transplantation for treating chronic obstructive pulmonary disease: a pilot clinical study. Stem Cell Research & Therapy, 11(1), p. 1-14. 8. Borzone, G., Liberona, L., Olmos, P., Sáez, C., Meneses, M., Reyes, T., Moreno, R. & Lisboa, C. (2007). Rat and hamster species differences in susceptibility to elastase-induced pulmonary emphysema relate to differences in elastase inhibitory capacity. American Journal of Physiology-Regulatory, Integrative and Comparative Physiology, 293(3), p. R1342-R1349. 9. Burgel, P. & Martin, C. (2010). Mucus hypersecretion in COPD: should we only rely on symptoms? : Eur Respiratory Soc. 10. Caramori, G., Romagnoli, M., Casolari, P., Bellettato, C., Casoni, G., Boschetto, P., Chung, K. F., Barnes, P., Adcock, I. & Ciaccia, A. (2003). Nuclear localisation of p65 in sputum macrophages but not in sputum neutrophils during COPD exacerbations. Thorax, 58(4), p. 348-351. 11. Celli, B. R., MacNee, W. & Force, A. E. T. (2004). Standards for the diagnosis and treatment of patients with COPD: a summary of the ATS/ERS position paper. Eur Respir J, 23(6), p. 932-46. 12. Churg, A., Cosio, M. & Wright, J. L. (2008). Mechanisms of cigarette smoke-induced COPD: insights from animal models. Am J Physiol Lung Cell Mol Physiol, 294(4), p. L612-31. 13. Churg, A., Wang, R. D., Tai, H., Wang, X., Xie, C., Dai, J., Shapiro, S. D. & Wright, J. L. (2003). Macrophage metalloelastase mediates acute cigarette smoke–induced inflammation via tumor necrosis factor-α release. American journal of respiratory and critical care medicine, 167(8), p. 1083-1089. 14. D'Agostino, B., Sullo, N., Siniscalco, D., De Angelis, A. & Rossi, F. (2010). Mesenchymal stem cell therapy for the treatment of chronic obstructive pulmonary disease. Expert Opin Biol Ther, 10(5), p. 681-7. 15. de Castro, L. L., Xisto, D. G., Kitoko, J. Z., Cruz, F. F., Olsen, P. C., Redondo, P. A. G., Ferreira, T. P. T., Weiss, D. J., Martins, M. A. & Morales, M. M. (2017). Human adipose tissue mesenchymal stromal cells and their extracellular vesicles act differentially on lung mechanics and inflammation in experimental allergic asthma. Stem cell research & therapy, 8(1), p. 151. 16. de Oliveira, M. V. (2016). Animal Models of Chronic Obstructive Pulmonary Disease Exacerbations: A Review of the Current Status. Journal of Biomedical Sciencies, 05(01), p. 17. Di Stefano, A., Caramori, G., Oates, T., Capelli, A., Lusuardi, M., Gnemmi, I., Ioli, F., Chung, K. F., Donner, C. F., Barnes, P. J. & Adcock, I. M. (2002). Increased expression of nuclear factor- B in bronchial biopsies from smokers and patients with COPD. European Respiratory Journal, 20(3), p. 556-563. 18. Diaz-Meco, M. T. & Moscat, J. (2012). The atypical PKCs in inflammation: NF-κB and beyond. Immunological reviews, 246(1), p. 154-167. 19. Dominici, M., Le Blanc, K., Mueller, I., Slaper-Cortenbach, I., Marini, F., Krause, D., Deans, R., Keating, A., Prockop, D. & Horwitz, E. (2006). Minimal criteria for defining multipotent mesenchymal stromal cells. The International Society for Cellular Therapy position statement. Cytotherapy, 8(4), p. 315-317. 20. Dong, L. H., Jiang, Y. Y., Liu, Y. J., Cui, S., Xia, C. C., Qu, C., Jiang, X., Qu, Y. Q., Chang, P. Y. & Liu, F. (2015). The anti-fibrotic effects of mesenchymal stem cells on irradiated lungs via stimulating endogenous secretion of HGF and PGE2. Sci Rep, 5, p. 8713. 21. Etzrodt, M., Cortez-Retamozo, V., Newton, A., Zhao, J., Ng, A., Wildgruber, M., Romero, P., Wurdinger, T., Xavier, R., Geissmann, F., Meylan, E., Nahrendorf, M., Swirski, F. K., Baltimore, D., Weissleder, R. & Pittet, M. J. (2012). Regulation of monocyte functional heterogeneity by miR-146a and Relb. Cell Rep, 1(4), p. 317-24. 22. Fischer, B. M. & Voynow, J. A. (2002). Neutrophil elastase

induces MUC 5AC gene expression in airway epithelium via a pathway involving reactive oxygen species. American journal of respiratory cell and molecular biology, 26(4), p. 447-452. 23. Flouris, A. D., Poulianiti, K. P., Chorti, M. S., Jamurtas, A. Z., Kouretas, D., Owolabi, E. O., Tzatzarakis, M. N., Tsatsakis, A. M. & Koutedakis, Y. (2012). Acute effects of electronic and tobacco cigarette smoking on complete blood count. Food and chemical toxicology, 50(10), p. 3600-3603. 24. Fontaine, M. J., Shih, H., Schäfer, R. & Pittenger, M. F. (2016). Unraveling the mesenchymal stromal cells' paracrine immunomodulatory effects. Transfusion medicine reviews, 30(1), p. 37-43. 25. Fujisawa, T., Chang, M. M.-J., Velichko, S., Thai, P., Hung, L.-Y., Huang, F., Phuong, N., Chen, Y. & Wu, R. (2011). NF-κB mediates IL-1β–and IL-17A–induced MUC5B expression in airway epithelial cells. American journal of respiratory cell and molecular biology, 45(2), p. 246-252. 26. Ghorani, V., Boskabady, M. H., Khazdair, M. R. & Kianmeher, M. (2017). Experimental animal models for COPD: a methodological review. Tob Induc Dis, 15, p. 25. 27. Giridharan, S. & Srinivasan, M. (2018). Mechanisms of NF-κB p65 and strategies for therapeutic manipulation. Journal of inflammation research, 11, p. 407. 28. Gonzalez-Rey, E., Gonzalez, M. A., Varela, N., O'Valle, F., Hernandez-Cortes, P., Rico, L., Buscher, D. & Delgado, M. (2010). Human adipose-derived mesenchymal stem cells reduce inflammatory and T cell responses and induce regulatory T cells in vitro in rheumatoid arthritis. Ann Rheum Dis, 69(1), p. 241-8. 29. Greening, D. W., Xu, R., Ji, H., Tauro, B. J. & Simpson, R. J. (2015). A protocol for exosome isolation and characterization: evaluation of ultracentrifugation, density-gradient separation, and immunoaffinity capture methods. Methods Mol Biol, 1295, p. 179-209. 30. Gu, W., Song, L., Li, X. M., Wang, D., Guo, X. J. & Xu, W. G. (2015). Mesenchymal stem cells alleviate airway inflammation and emphysema in COPD through down-regulation of cyclooxygenase-2 via p38 and ERK MAPK pathways. Sci Rep, 5, p. 8733. 31. Guan, X. J., Song, L., Han, F. F., Cui, Z. L., Chen, X., Guo, X. J. & Xu, W. G. (2013). Mesenchymal stem cells protect cigarette smoke-damaged lung and pulmonary function partly via VEGF-VEGF receptors. J Cell Biochem, 114(2), p. 323-35. 32. Hayes, J., Schuster, M., Grossman, F., Rutman, O. & Itescu, S. (2020). Mesenchymal stem cell therapy improves pulmonary function and exercise tolerance in patients with chronic obstructive pulmonary disease (copd) and high baseline inflammation. Cytotherapy, 22(5), p. S188-S189. 33. He, F., Liao, B., Pu, J., Li, C., Zheng, M., Huang, L., Zhou, Y., Zhao, D., Li, B. & Ran, P. (2017). Exposure to ambient particulate matter induced COPD in a rat model and a description of the underlying mechanism. Scientific reports, 7, p. 45666. 34. He, Z. H., Chen, P., Chen, Y., He, S. D., Ye, J. R., Zhang, H. L. & Cao, J. (2015). Comparison between cigarette smoke-induced emphysema and cigarette smoke extract-induced emphysema. Tob Induc Dis, 13(1), p. 6. 35. Hou, H.-H., Cheng, S.-L., Chung, K.-P., Wei, S.-C., Tsao, P.-N., Lu, H.-H., Wang, H.-C. & Yu, C.-J. (2014). PlGF mediates neutrophil elastase-induced airway epithelial cell apoptosis and emphysema. Respiratory research, 15(1), p. 106. 36. Huh, J. W., Kim, S. Y., Lee, J. H., Lee, J. S., Van Ta, Q., Kim, M., Oh, Y. M., Lee, Y. S. & Lee, S. D. (2011). Bone marrow cells repair cigarette smoke-induced emphysema in rats. Am J Physiol Lung Cell Mol Physiol, 301(3), p. L255-66. 37. Jin, H. J., Bae, Y. K., Kim, M., Kwon, S.-J., Jeon, H. B., Choi, S. J., Kim, S. W., Yang, Y. S., Oh, W. & Chang, J. W. (2013). Comparative analysis of human mesenchymal stem cells from bone marrow, adipose tissue, and umbilical cord blood as sources of cell therapy. International journal of molecular sciences, 14(9), p. 17986-18001. 38. Kadota, T., Fujita, Y., Yoshioka, Y., Araya, J., Kuwano, K. & Ochiya, T. (2016). Extracellular vesicles in chronic obstructive pulmonary disease. International journal of molecular sciences, 17(11), p. 1801. 39. Kim, Y.-S., Kim, J.-Y.,

Cho, R., Shin, D.-M., Lee, S. W. & Oh, Y.-M. (2017). Adipose stem cell-derived nanovesicles inhibit emphysema primarily via an FGF2-dependent pathway. Experimental & molecular medicine, 49(1), p. e284-e284. 40. Kim, Y. S., Kokturk, N., Kim, J. Y., Lee, S. W., Lim, J., Choi, S. J., Oh, W. & Oh, Y. M. (2016). Gene Profiles in a Smoke-Induced COPD Mouse Lung Model Following Treatment with Mesenchymal Stem Cells. Mol Cells, 39(10), p. 728-733. 41. Kohri, K., Ueki, I. F. & Nadel, J. A. (2002). Neutrophil elastase induces mucin production by ligand-dependent epidermal growth factor receptor activation. American Journal of Physiology-Lung Cellular and Molecular Physiology, 283(3), p. L531-L540. 42. Lai, R. C., Arslan, F., Lee, M. M., Sze, N. S., Choo, A., Chen, T. S., Salto-Tellez, M., Timmers, L., Lee, C. N., El Oakley, R. M., Pasterkamp, G., de Kleijn, D. P. & Lim, S. K. (2010). Exosome secreted by MSC reduces myocardial ischemia/reperfusion injury. Stem Cell Res, 4(3), p. 214-22. 43. Leberl, M., Kratzer, A. & Taraseviciene-Stewart, L. (2013). Tobacco smoke induced COPD/emphysema in the animal model-are we all on the same page? Front Physiol, 4, p. 91. 44. Lee, C., Mitsialis, S. A., Aslam, M., Vitali, S. H., Vergadi, E., Konstantinou, G., Sdrimas, K., Fernandez-Gonzalez, A. & Kourembanas, S. (2012). Exosomes mediate the cytoprotective action of mesenchymal stromal cells on hypoxia-induced pulmonary hypertension. Circulation, 126(22), p. 2601-11. 45. Lee, S.-H., Jang, A.-S., Kwon, J.-H., Park, S.-K., Won, J.-H. & Park, C.-S. (2011). Mesenchymal stem cell transfer suppresses airway remodeling in a toluene diisocyanate-induced murine asthma model. Allergy, asthma & immunology research, 3(3), p. 205-211. 46. Li, X., Wang, J., Cao, J., Ma, L. & Xu, J. (2015). Immunoregulation of Bone Marrow-Derived Mesenchymal Stem Cells on the Chronic Cigarette Smoking-Induced Lung Inflammation in Rats. Biomed Res Int, 2015, p. 932923. 47. Liu, T., Zhang, L., Joo, D. & Sun, S.-C. (2017). NF-κB signaling in inflammation. Signal transduction and targeted therapy, 2(1), p. 1-9. 48. Liu, X., Fang, Q. & Kim, H. (2016). Preclinical studies of mesenchymal stem cell (MSC) administration in chronic obstructive pulmonary disease (COPD): a systematic review and meta-analysis. PLoS One, 11(6), p. 49. Ludwig, A. K. & Giebel, B. (2012). Exosomes: small vesicles participating in intercellular communication. Int J Biochem Cell Biol, 44(1), p. 11-5. 50. Mathias, L. J., Khong, S. M., Spyroglou, L., Payne, N. L., Siatskas, C., Thorburn, A. N., Boyd, R. L. & Heng, T. S. (2013). Alveolar macrophages are critical for the inhibition of allergic asthma by mesenchymal stromal cells. J Immunol, 191(12), p. 5914-24. 51. Mohammadian, M., Boskabady, M. H., Kashani, I. R., Jahromi, G. P., Omidi, A., Nejad, A. K., Khamse, S. & Sadeghipour, H. R. (2016). Effect of bone marrow derived mesenchymal stem cells on lung pathology and inflammation in ovalbumin-induced asthma in mouse. Iranian journal of basic medical sciences, 19(1), p. 55. 52. Nie, Y.-C., Wu, H., Li, P.-B., Luo, Y.-L., Zhang, C.-C., Shen, J.-G. & Su, W.-W. (2012). Characteristic comparison of three rat models induced by cigarette smoke or combined with LPS: to establish a suitable model for study of airway mucus hypersecretion in chronic obstructive pulmonary disease. Pulmonary pharmacology & therapeutics, 25(5), p. 349-356. 53. O'Farrell, H. E. & Yang, I. A. (2019). Extracellular vesicles in chronic obstructive pulmonary disease (COPD). Journal of thoracic disease, 11(Suppl 17), p. S2141. 54. Panes, J., Garcia-Olmo, D., Van Assche, G., Colombel, J. F., Reinisch, W., Baumgart, D. C., Dignass, A., Nachury, M., Ferrante, M., Kazemi-Shirazi, L., Grimaud, J. C., de la Portilla, F., Goldin, E., Richard, M. P., Leselbaum, A., Danese, S. & Collaborators, A. C. S. G. (2016). Expanded allogeneic adipose-derived mesenchymal stem cells (Cx601) for complex perianal fistulas in Crohn's disease: a phase 3 randomised, double-blind controlled trial. Lancet, 388(10051), p. 1281-90. 55. Phinney, D. G., Di Giuseppe, M., Njah, J., Sala, E., Shiva, S., St Croix, C. M., Stolz, D. B., Watkins, S. C., Di, Y.

P. & Leikauf, G. D. (2015). Mesenchymal stem cells use extracellular vesicles to outsource mitophagy and shuttle microRNAs. Nature communications, 6, p. 8472. 56. Presson Jr, R. G., Brown, M. B., Fisher, A. J., Sandoval, R. M., Dunn, K. W., Lorenz, K. S., Delp, E. J., Salama, P., Molitoris, B. A. & Petrache, I. (2011). Two-photon imaging within the murine thorax without respiratory and cardiac motion artifact. The American journal of pathology, 179(1), p. 75-82. 57. Rani, S., Ryan, A. E., Griffin, M. D. & Ritter, T. (2015). Mesenchymal Stem Cell-derived Extracellular Vesicles: Toward Cell-free Therapeutic Applications. Mol Ther, 23(5), p. 812-823. 58. Sarko, D. K. & McKinney, C. E. (2017). Exosomes: Origins and Therapeutic Potential for Neurodegenerative Disease. Front Neurosci, 11, p. 82. 59. Schweitzer, K. S., Hatoum, H., Brown, M. B., Gupta, M., Justice, M. J., Beteck, B., Van Demark, M., Gu, Y., Presson Jr, R. G. & Hubbard, W. C. (2011). Mechanisms of lung endothelial barrier disruption induced by cigarette smoke: role of oxidative stress and ceramides. American Journal of Physiology-Lung Cellular and Molecular Physiology, 301(6), p. L836-L846. 60. Shao, M. X., Nakanaga, T. & Nadel, J. A. (2004). Cigarette smoke induces MUC5AC mucin overproduction via tumor necrosis factor-α-converting enzyme in human airway epithelial (NCI-H292) cells. American Journal of Physiology-Lung Cellular and Molecular Physiology, 287(2), p. L420-L427. 61. Shapiro, S. D. (1999). The macrophage in chronic obstructive pulmonary disease. Am J Respir Crit Care Med, 160(5 Pt 2), p. S29-32. 62. Shapiro, S. D., Goldstein, N. M., Houghton, A. M., Kobayashi, D. K., Kelley, D. & Belaaouaj, A. (2003). Neutrophil elastase contributes to cigarette smoke-induced emphysema in mice. The American journal of pathology, 163(6), p. 2329-2335. 63. Shen, B., Liu, J., Zhang, F., Wang, Y., Qin, Y., Zhou, Z., Qiu, J. & Fan, Y. (2016). CCR2 positive exosome released by mesenchymal stem cells suppresses macrophage functions and alleviates ischemia/reperfusion-induced renal injury. Stem cells international, 2016, p. 64. Sicco, C. L., Reverberi, D., Balbi, C., Ulivi, V., Principi, E., Pascucci, L., Becherini, P., Bosco, M. C., Varesio, L. & Franzin, C. (2017). Mesenchymal stem cell-derived extracellular vesicles as mediators of anti-inflammatory effects: Endorsement of macrophage polarization. Stem cells translational medicine, 6(3), p. 1018-1028. 65. Song, X., Xie, S., Lu, K. & Wang, C. (2015). Mesenchymal stem cells alleviate experimental asthma by inducing polarization of alveolar macrophages. Inflammation, 38(2), p. 485-92. 66. Stevenson, C. S., Docx, C., Webster, R., Battram, C., Hynx, D., Giddings, J., Cooper, P. R., Chakravarty, P., Rahman, I., Marwick, J. A., Kirkham, P. A., Charman, C., Richardson, D. L., Nirmala, N. R., Whittaker, P. & Butler, K. (2007). Comprehensive gene expression profiling of rat lung reveals distinct acute and chronic responses to cigarette smoke inhalation. Am J Physiol Lung Cell Mol Physiol, 293(5), p. L1183-93. 67. Stone, M. L., Zhao, Y., Smith, J. R., Weiss, M. L., Kron, I. L., Laubach, V. E. & Sharma, A. K. (2017). Mesenchymal stromal cell-derived extracellular vesicles attenuate lung ischemia-reperfusion injury and enhance reconditioning of donor lungs after circulatory death. Respiratory research, 18(1), p. 212. 68. Tan, C., Xuan, L., Cao, S., Yu, G., Hou, Q. & Wang, H. (2016). Decreased histone deacetylase 2 (HDAC2) in peripheral blood monocytes (PBMCs) of COPD patients. PLoS One, 11(1), p. 69. Weiss, D. J., Casaburi, R., Flannery, R., LeRoux-Williams, M. & Tashkin, D. P. (2013). A placebo-controlled, randomized trial of mesenchymal stem cells in COPD. Chest, 143(6), p. 1590-1598. 70. Witwer, K. W., Van Balkom, B. W., Bruno, S., Choo, A., Dominici, M., Gimona, M., Hill, A. F., De Kleijn, D., Koh, M. & Lai, R. C. (2019). Defining mesenchymal stromal cell (MSC)-derived small extracellular vesicles for therapeutic applications. Journal of extracellular vesicles, 8(1), p. 1609206. 71. Yan, Y., Jiang, W., Tan, Y., Zou, S., Zhang, H., Mao, F., Gong, A., Qian, H. & Xu, W. (2017). hucMSC exosome-derived GPX1 is required for the

recovery of hepatic oxidant injury. Molecular Therapy, 25(2), p. 465-479. 72. Yang, J., Jin, J., Zhang, Z., Zhang, L. & Shen, C. (2013). Integration microarray and regulation datasets for chronic obstructive pulmonary disease. Eur Rev Med Pharmacol Sci, 17(14), p. 1923-1931. 73. Yang, J., Liu, X.-X., Fan, H., Tang, Q., Shou, Z.-X., Zuo, D.-M., Zou, Z., Xu, M., Chen, Q.-Y. & Peng, Y. (2015). Extracellular vesicles derived from bone marrow mesenchymal stem cells protect against experimental colitis via attenuating colon inflammation, oxidative stress and apoptosis. PloS one, 10(10), p. 74. Yao, H., Hwang, J.-w., Moscat, J., Diaz-Meco, M. T., Leitges, M., Kishore, N., Li, X. & Rahman, I. (2010). Protein kinase Cζ mediates cigarette smoke/aldehyde-and lipopolysaccharide-induced lung inflammation and histone modifications. Journal of Biological Chemistry, 285(8), p. 5405-5416. 75. Yao, J., Zheng, J., Cai, J., Zeng, K., Zhou, C., Zhang, J., Li, S., Li, H., Chen, L. & He, L. (2019). Extracellular vesicles derived from human umbilical cord mesenchymal stem cells alleviate rat hepatic ischemia-reperfusion injury by suppressing oxidative stress and neutrophil inflammatory response. The FASEB Journal, 33(2), p. 1695-1710. 76. Yu, B., Zhang, X. & Li, X. (2014). Exosomes derived from mesenchymal stem cells. Int J Mol Sci, 15(3), p. 4142-57. 77. Yu, D., Liu, X., Zhang, G., Ming, Z. & Wang, T. (2018). Isoliquiritigenin inhibits cigarette smoke-induced COPD by attenuating inflammation and oxidative stress via the regulation of the Nrf2 and NF-κB signaling pathways. Frontiers in pharmacology, 9, p. 1001. 78. Zeng, S. L., Wang, L. H., Li, P., Wang, W. & Yang, J. (2015). Mesenchymal stem cells abrogate experimental asthma by altering dendritic cell function. Mol Med Rep, 12(2), p. 2511-20. 79. Zhang, W.-G., He, L., Shi, X.-M., Wu, S.-S., Zhang, B., Mei, L., Xu, Y.-J., Zhang, Z.-X., Zhao, J.-P. & Zhang, H.-L. (2014). Regulation of transplanted mesenchymal stem cells by the lung progenitor niche in rats with chronic obstructive pulmonary disease. Respiratory research, 15(1), p. 33. 80. Zheng, H., Liu, Y., Huang, T., Fang, Z., Li, G. & He, S. (2009). Development and characterization of a rat model of chronic obstructive pulmonary disease (COPD) induced by sidestream cigarette smoke. Toxicol Lett, 189(3), p. 225-34. 81. Zhou, L., Liu, Y., Chen, X., Wang, S., Liu, H., Zhang, T., Zhang, Y., Xu, Q., Han, X. & Zhao, Y. (2018). Over-expression of nuclear factor-κB family genes and inflammatory molecules is related to chronic obstructive pulmonary disease. International journal of chronic obstructive pulmonary disease, 13, p. 2131. 82. Zhu, Y. g., Feng, X. m., Abbott, J., Fang, X. h., Hao, Q., Monsel, A., Qu, J. m., Matthay, M. A. & Lee, J. W. (2014). Human mesenchymal stem cell microvesicles for treatment of Escherichia coli endotoxin-induced acute lung injury in mice. Stem cells, 32(1), p. 116-125. 83. Zulueta, A., Colombo, M., Peli, V., Falleni, M., Tosi, D., Ricciardi, M., Baisi, A., Bulfamante, G., Chiaramonte, R. & Caretti, A. (2018). Lung mesenchymal stem cells-derived extracellular vesicles attenuate the inflammatory profile of cystic fibrosis epithelial cells. Cellular signalling, 51, p. 110-118.

Figures

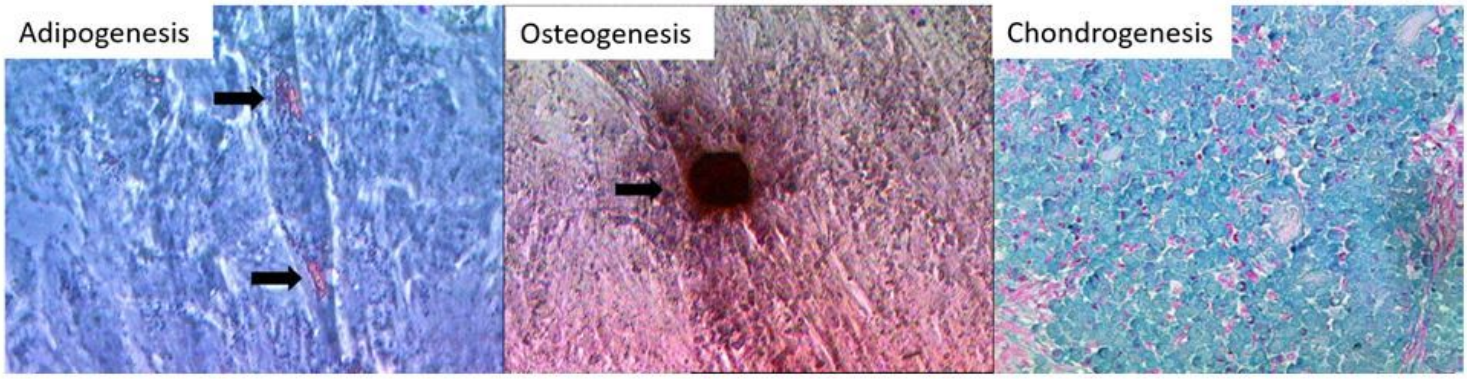

Figure 1

Differentiation of hUC-MSC. hUC-MSC differentiate into adipogenesis, osteogenesis, and chondrogenesis, under the differentiation medium. Adipogenesis were evidenced by formation of lipid droplet stained red, osteogenesis were evidenced by calcification stained red, and chondrogenesis were evidenced by formation of cell matrix stained blue.

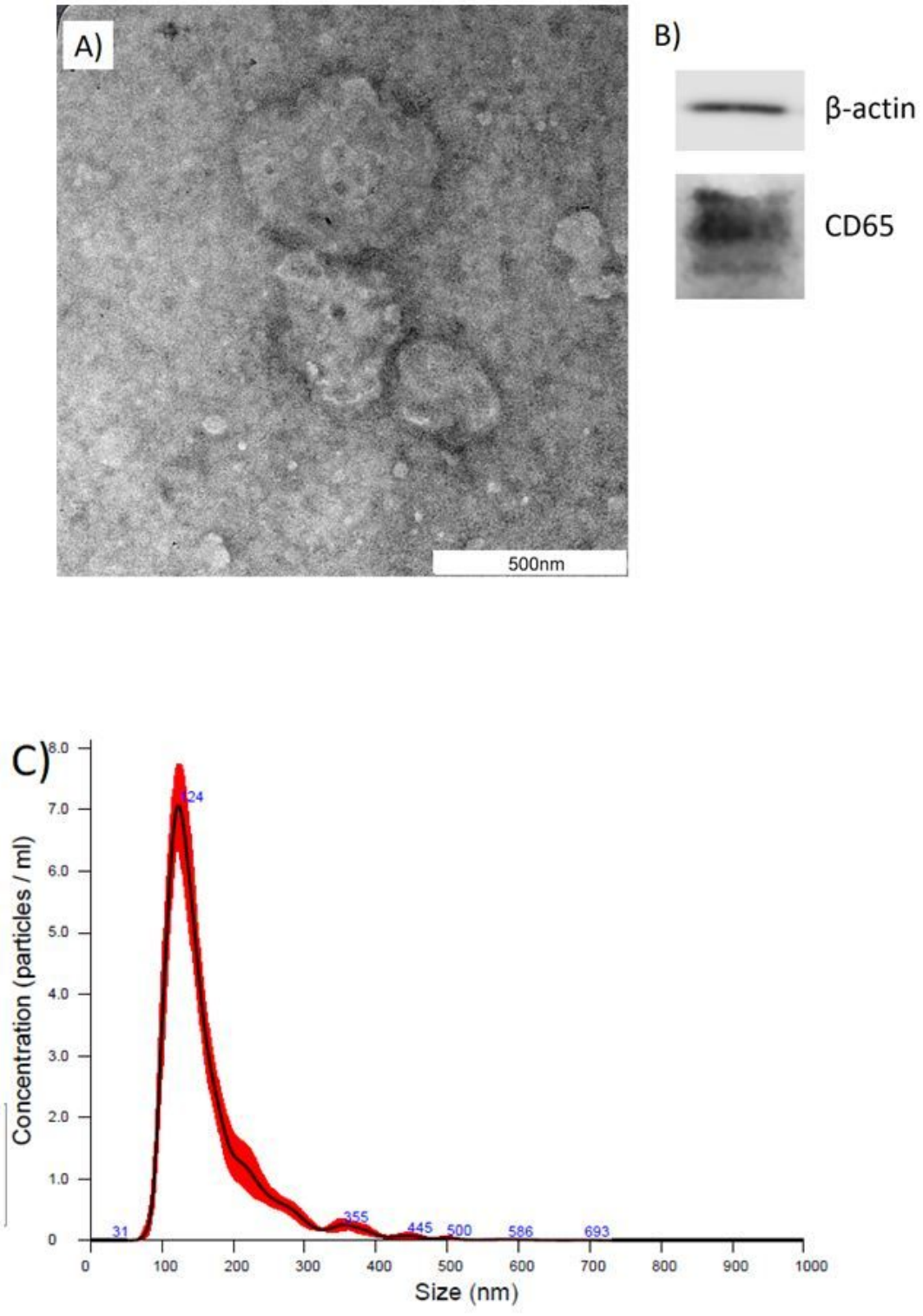

Figure 2

Characterization of hUC-MSC-EV. A) Morphological observation using EFTEM of hUC-MSC-EV showed to be rounded in shape. B) CD63 expression was observed by western blot analysis. β-actin is visible at 42kDa and CD65 is visible at 30-65kDa. C) Particle distribution by Nanosight NS300 reported an average hUC-MSC-EV diameter of 153nm. Representative data from three independent experiments.

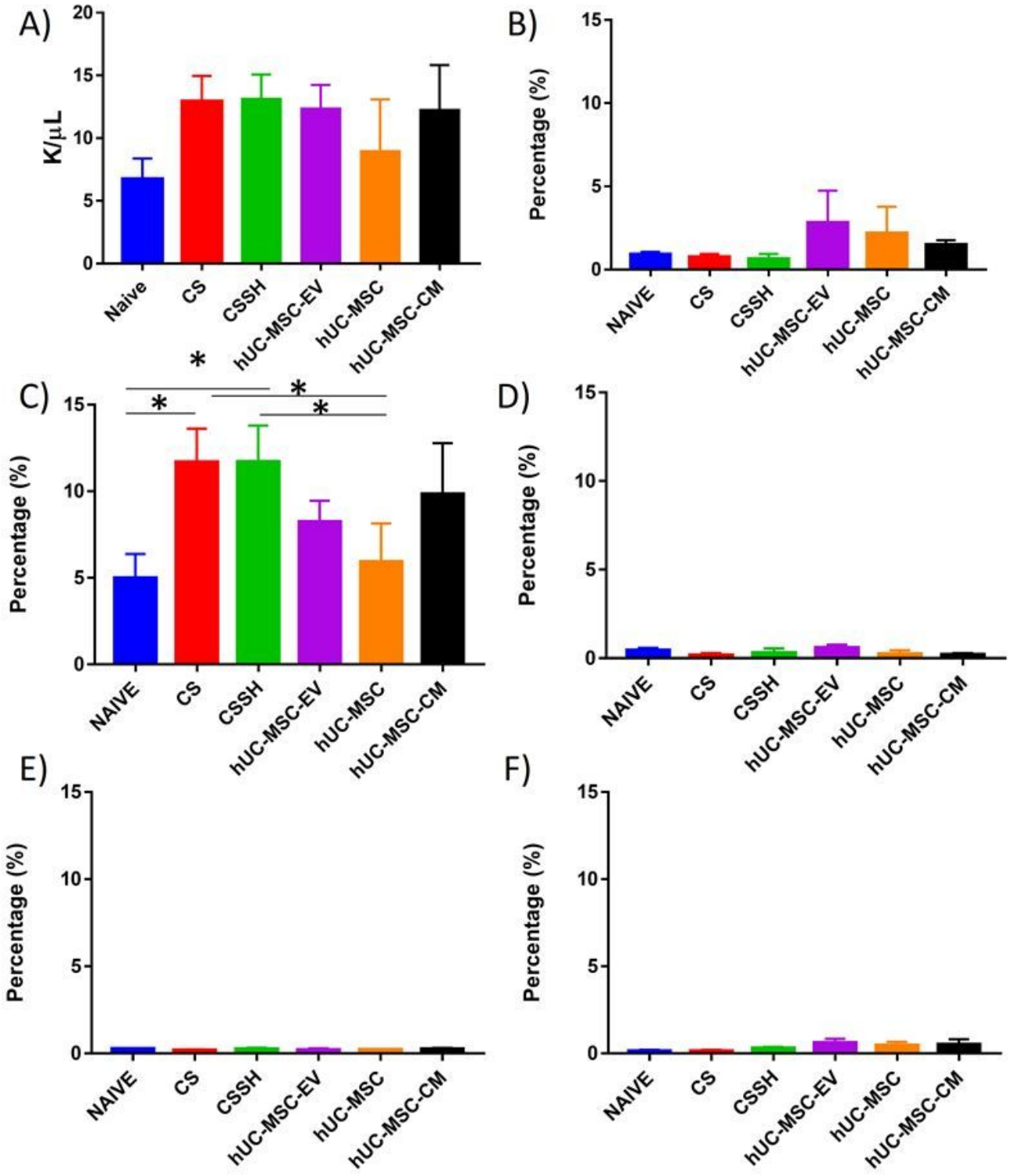

Figure 3

White blood and differential cell counts of peripheral blood in naïve and injury groups. A) White blood cell counts of peripheral blood in Naïve and CS groups show an increase in response to CS with no significant decrease following treatments. The following graphs show the differential cell counts for (B) neutrophils C) lymphocytes D) monocytes E) eosinophils D) basophils in peripheral blood. No significant increase of neutrophils, monocytes, eosinophils and basophils were observed in CS. However, the percentage of

lymphocytes significantly increased in response to CS followed by decrease following treatment with hUC-MSC-EV and hUC-MSC (*p<0.05). Data is median ± SD from n=3.

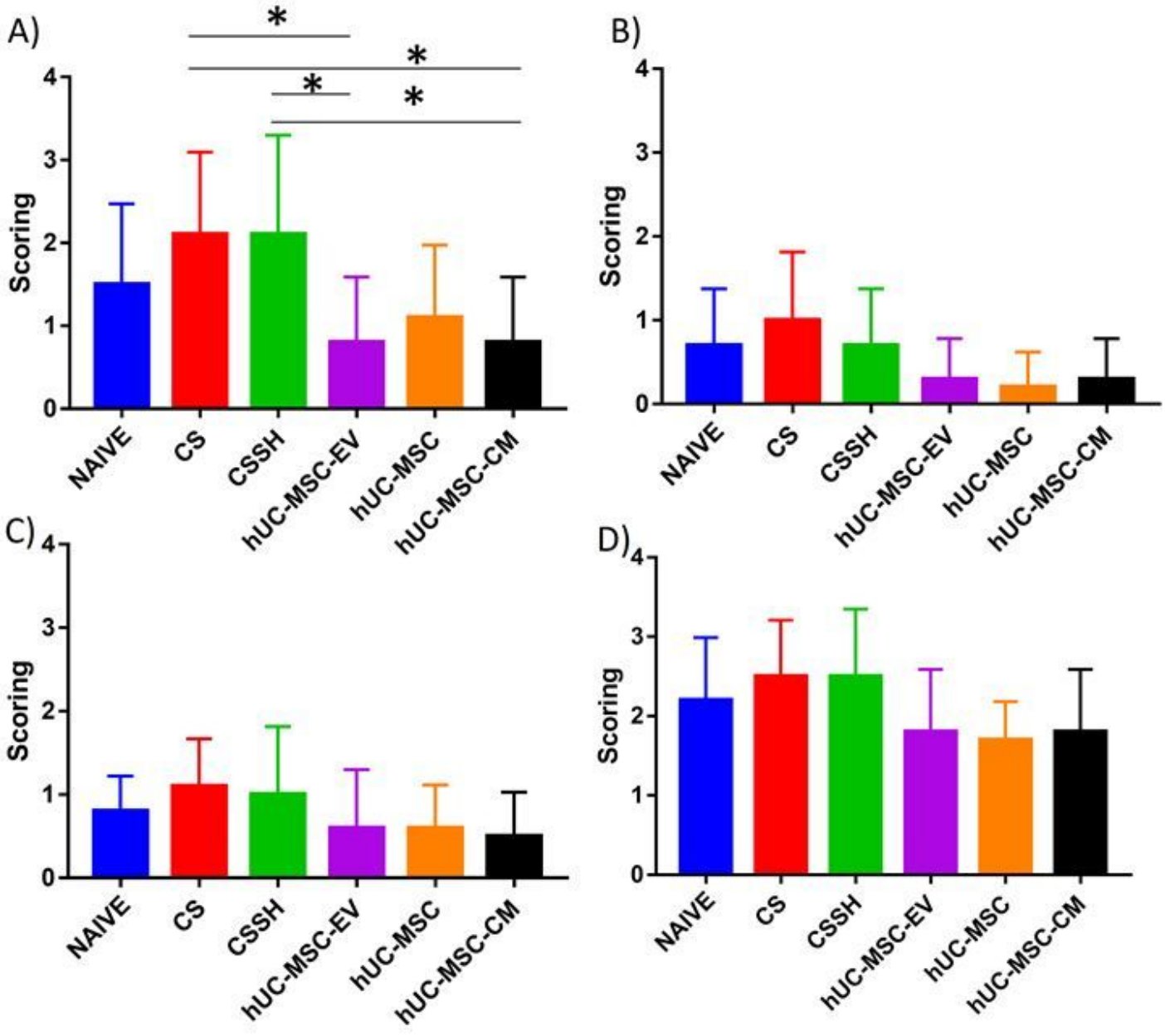

Figure 4

Infiltration of immune cells in rat lung. Semi-quantitative histological scoring and analysis of A) Neutrophils B) Eosinophils C) Lymphocytes D) Macrophages in the lung. CS increased the infiltration of neutrophils, eosinophils, lymphocytes, and macrophages into the lung. Two weeks of self-healing period (CSSH) failed to reduce the infiltration of all cells examined. Treatment with hUC-MSC-EV, and hUC-MSC-CM significantly (*p<0.05) reduced the infiltration of neutrophils. Data is median ± SD from n=5.

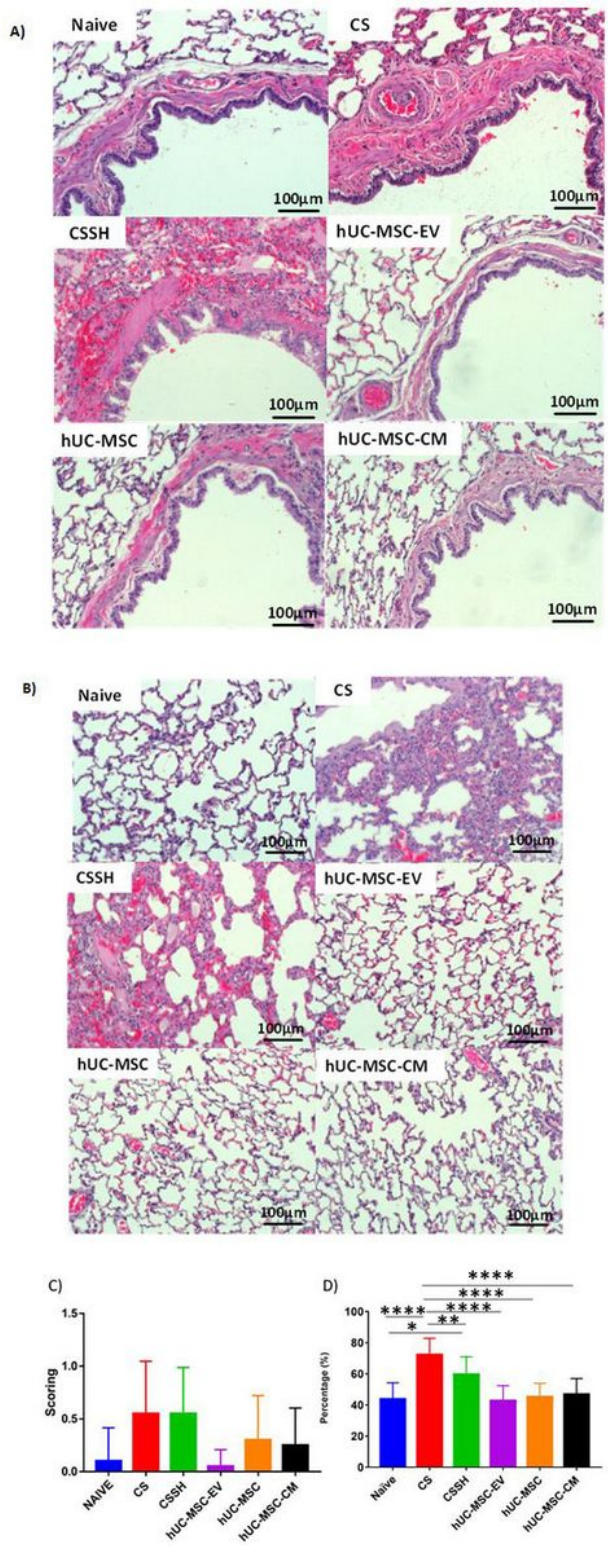

Figure 5

Airway and parenchyma inflammation in injury and treatment groups. Histological image of peribronchial (A) histological image of parenchyma (B) Semi-quantitative histological scoring and analysis of airway inflammation (C) and lung parenchymal inflammation (D). CS exposure over 12 weeks increased immune cell infiltration in the peribronchial, perivascular and alveolar area. Self-healing for 2 weeks (CSSH) did not reduce the inflammation. The scores for inflammation in the airway and alveolar area significantly

reduced following treatment with UCMSC-EV, hUC-MSC, and hUC-MSC-CM (****p< 0.0001) compared to the CS group. Data is median ± SD from n=5.

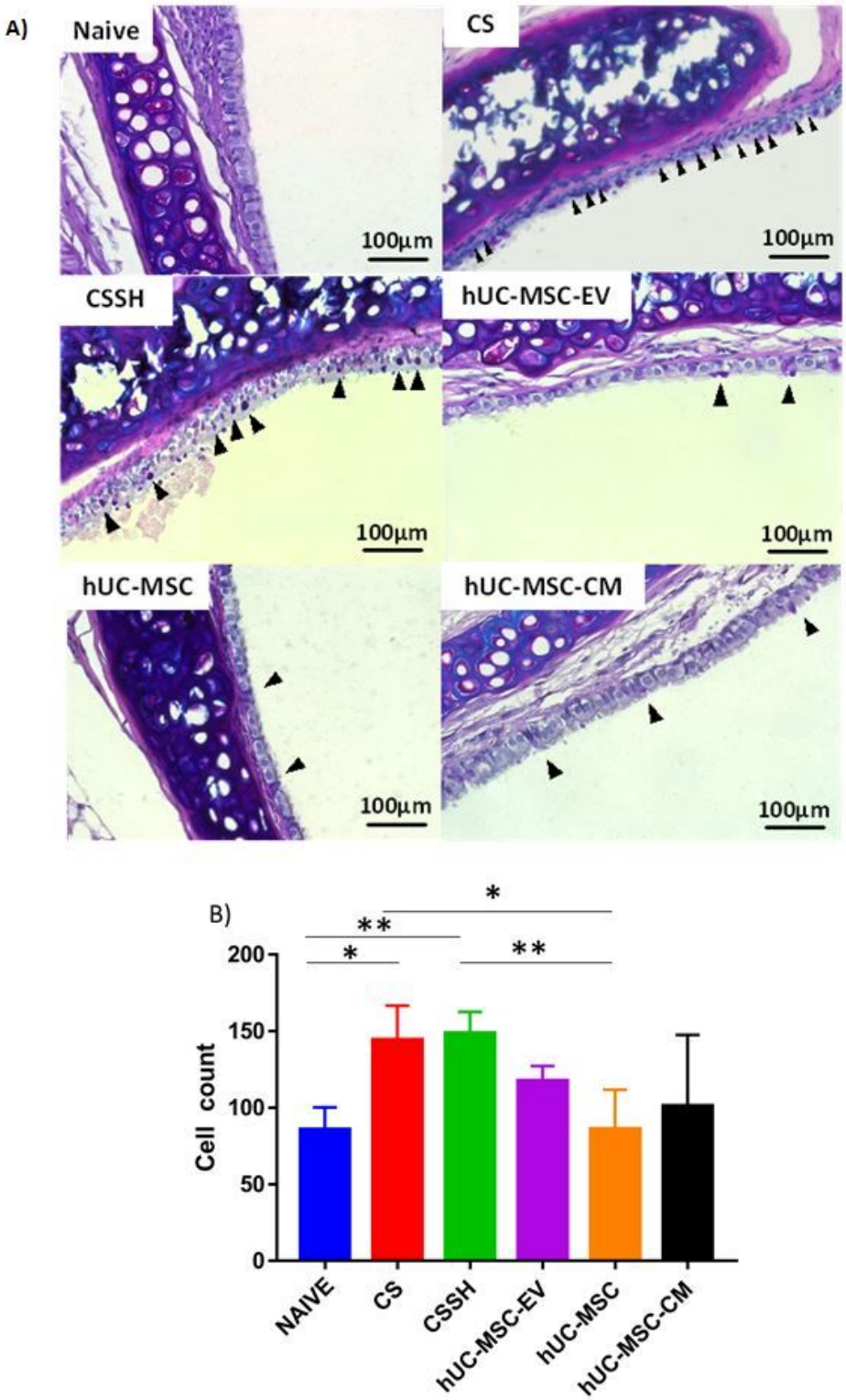

Figure 6

Goblet cell counts for the assessment of mucus overproduction. Quantitative histological staining (A) and analysis (B) of goblet cells within the bronchi. A significant increase in goblet cells was observed after 12 weeks of CS exposure with no reduction following 2 weeks of self-healing (CSSH). Treatment of

CS groups with MSC significantly reduced the number of goblet cells, and no-significant reduction in response to UCMSC-EV and UCMSC-CM. (*p<0.05, **p<0.001) Data is median ± SEM from n=5.

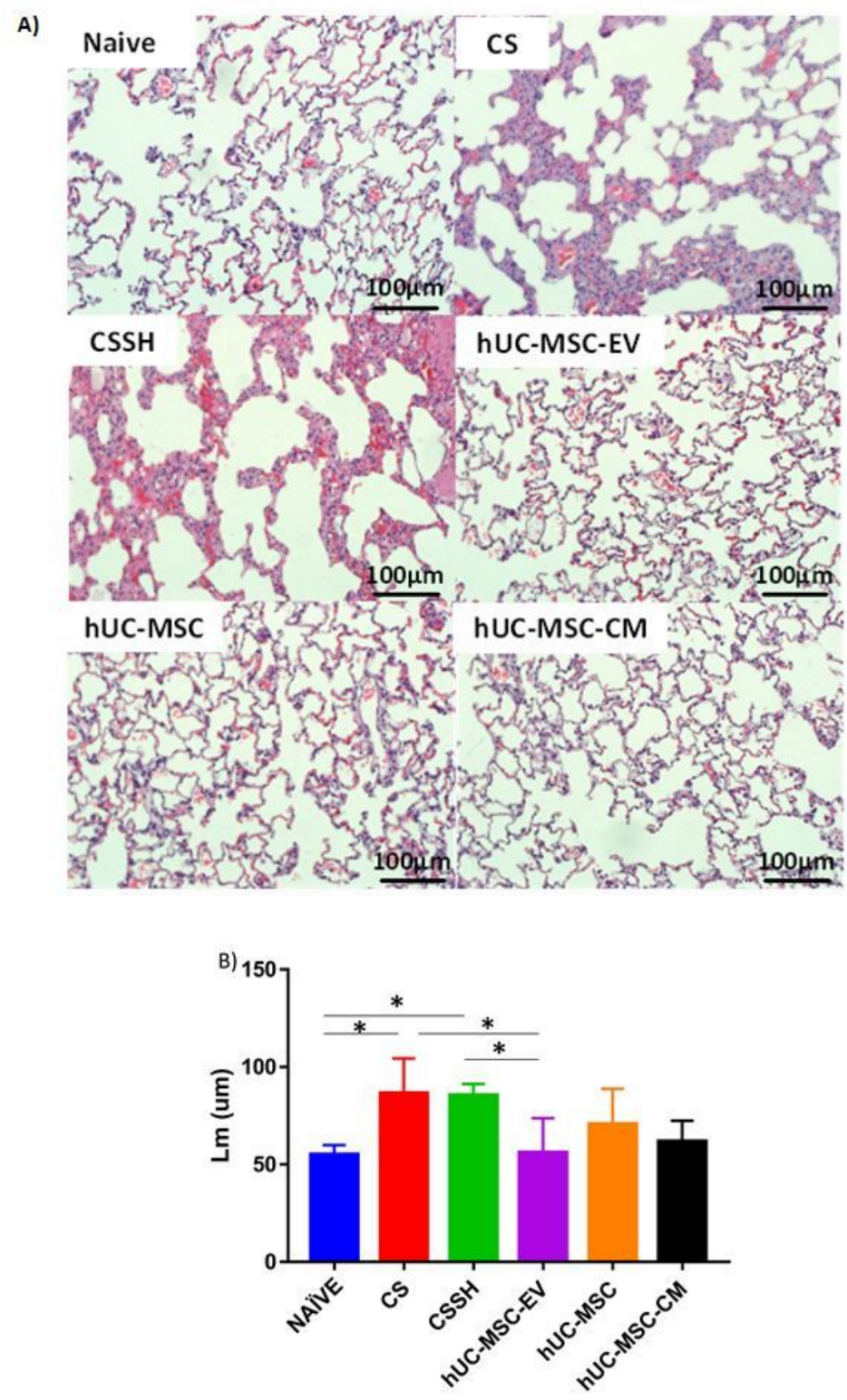

Figure 7

Mean linear intercept of cigarette smoke-exposed group. A) Representative histological sections stained with H&E staining for each group. B) Semi-quantitative analysis of mean linear intercept of CS-induced emphysema in rat lung. CS increased the mean linear intercept, and 2 weeks of self-healing failed to

alleviate the alveolar obstruction. Meanwhile, treatment with hUC-MSC-EV significantly reduced the mean linear intercept. hUC-MSC, and hUC-MSC-CM did not observe a significant reduction. *p<0.05. Data is median ± SD from n=5.

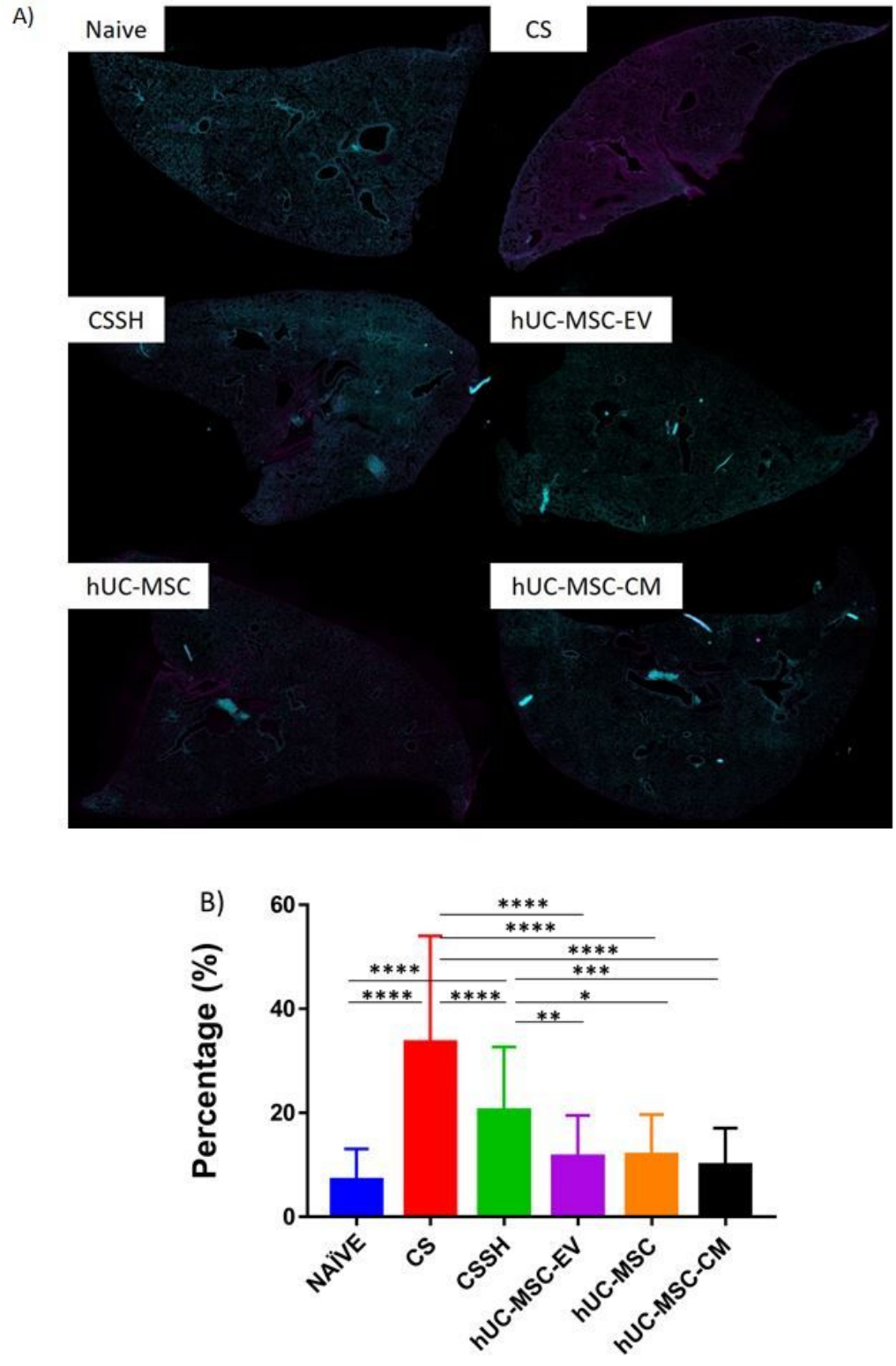

Figure 8

Immunofluorescence staining of CS exposed lung. Immunofluorescence staining was conducted to study the expression of A) p65 (purple) and dapi (turquoise) in the lung B) Percentage of p65 expression in all

groups. p65 expression was increased when exposed to CS, and smoking cessation for 2 weeks significantly reduced the expression of p65. The expression of p65 was further reduced when treated with hUC-MSC, hUC-MSC-EV, and hUC-MSC-CM. *p<0.05, **p<0.01, ****p<0.0001. Data is median ± SD from n=5.

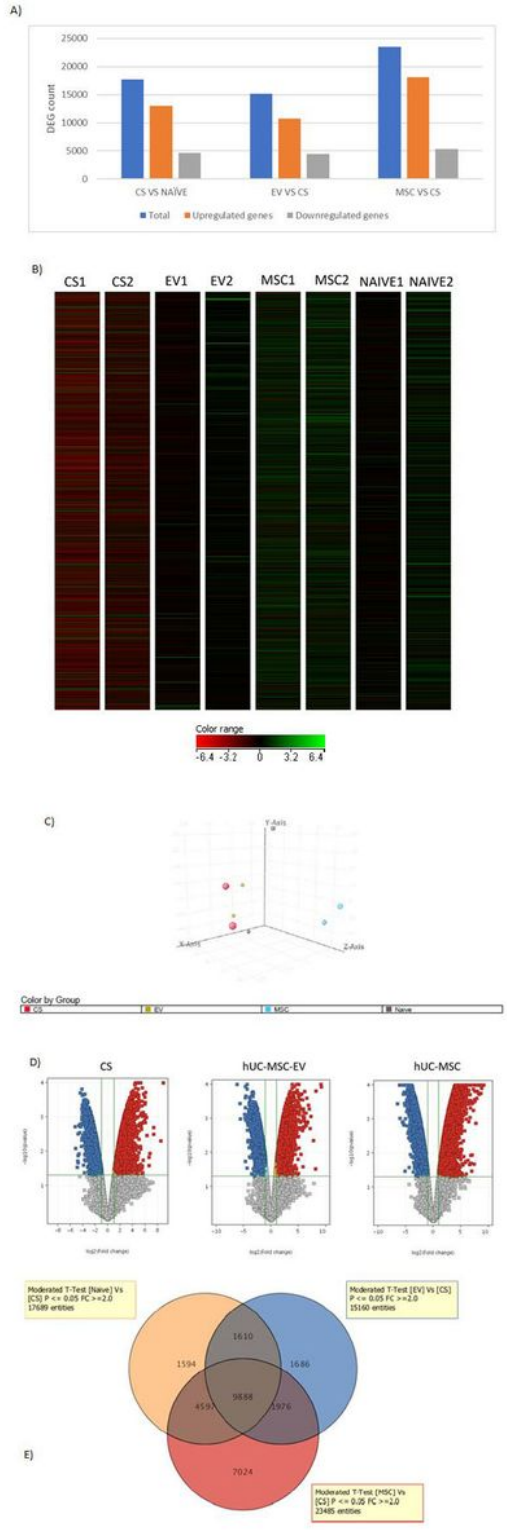

Figure 9

Microarray analysis of significantly regulated genes in CS exposed lung. A) The bar chart represents the total number of DEG, downregulated, and upregulated DEG with $p<0.05$ and $FC>2.0$ which considered significantly regulated. B) Heat map shows different DEG regulation in CS group as compared to Naïve, hUC-MSC-EV, and hUC-MSC group. C) PCA plot shows a cluster of samples (n=2) in Naïve, CS, hUC-MSC - EV, and hUC-MSC groups. D) Volcano plot of differentially expressed genes obtained from microarray analysis. The red dots represent upregulated DEG, while blue dots represent downregulated DEG. p-value generated using t-test. E) Venn diagram shows overlapping DEG among CS, hUC-MSC-EV, and hUC-MSC. 9888 DEG were overlapped in 3 groups, 1610 DEG were overlapped between CS and hUC-MSC-EV, 4597 DEG were overlapped between CS and hUC-MSC, and 1976 DEG were overlapped between hUC-MSC-EV and hUC-MSC.

Supplementary Files

This is a list of supplementary files associated with this preprint. Click to download.

- Suppltable.doc